NASA Technical Paper 3025

March 1991

Physically Weighted Approximations of Unsteady Aerodynamic Forces Using the Minimum-State Method

Mordechay Karpel and
Sherwood Tiffany Hoadley

NASA

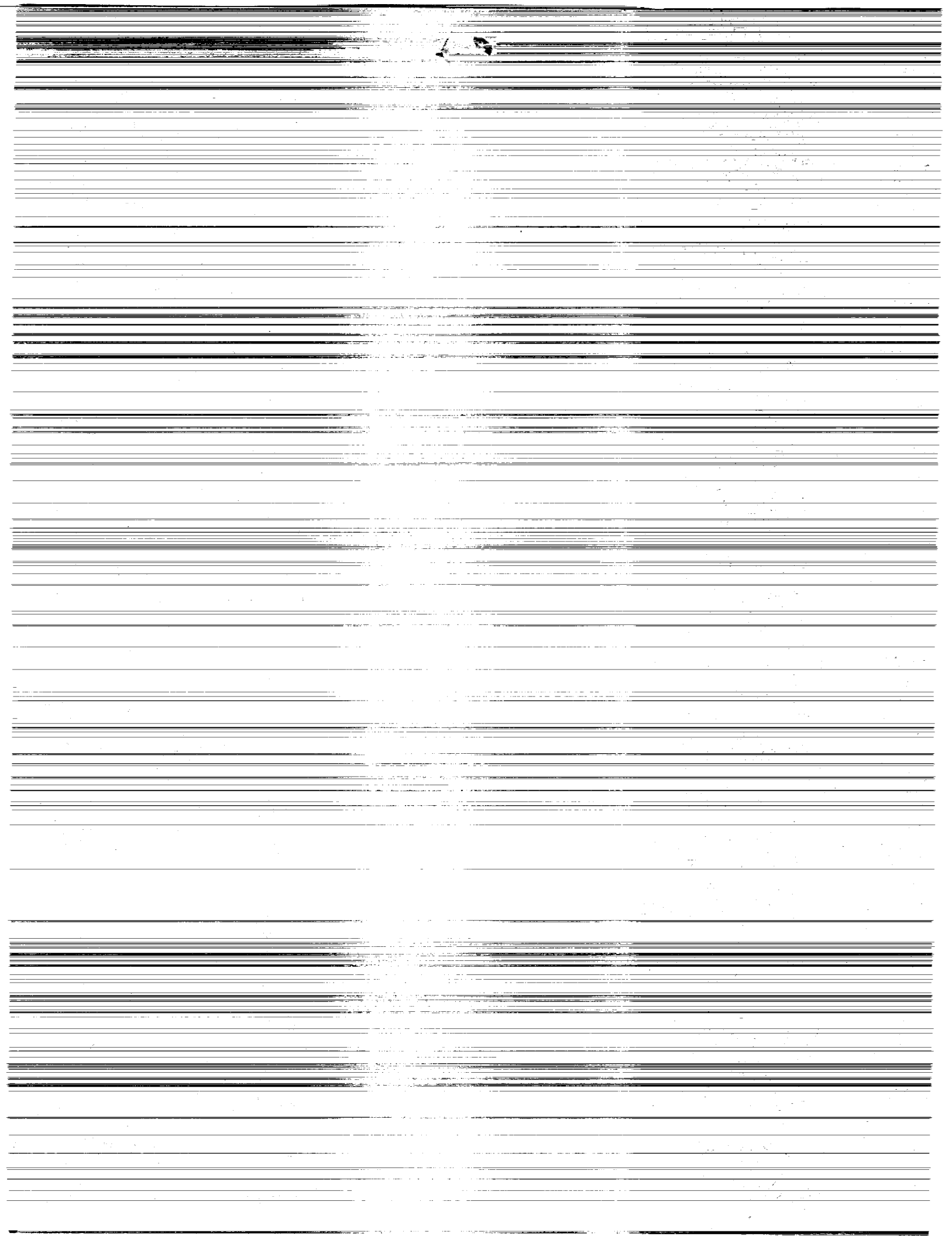

NASA Technical Paper 3025

1991

Physically Weighted Approximations of Unsteady Aerodynamic Forces Using the Minimum-State Method

Mordechay Karpel and
Sherwood Tiffany Hoadley
Langley Research Center
Hampton, Virginia

National Aeronautics and Space Administration
Office of Management
Scientific and Technical Information Division

Contents

Summary

The minimum-state method for rational approximation of unsteady aerodynamic force coefficient matrices, modified to allow physical weighting of the tabulated aerodynamic data, is presented. The approximation formula and the associated time-domain, state-space open-loop equations of motion are given, and the numerical procedures for calculating the approximation matrices, with weighted data and with various equality constraints, are described. Two data weighting options are presented. The first weighting is for normalizing the aerodynamic data to the maximum unit value of each aerodynamic coefficient. The second weighting is one in which each tabulated coefficient, at each reduced frequency value, is weighted according to the effect of an incremental error of this coefficient on aeroelastic characteristics of the system. This weighting yields a better fit of the more important terms at the expense of less important ones. The resulting approximation yields a relatively low number of aerodynamic lag states in the subsequent state-space model.

The formulation of this work forms the basis of the Minimum-State (MIST) computer program that is written in FORTRAN-77 for use on the VAX microcomputer and interfaces with NASA's Interaction of Structures, Aerodynamics, and Controls (ISAC) computer program. The program structure, capabilities, and interfaces are outlined in the appendixes, and a numerical example that utilizes Rockwell's Active Flexible Wing (AFW) model is given and discussed.

1. Introduction

Various control analysis, design, and simulation techniques of aeroservoelastic systems require the equations of motion to be cast in a linear, time-invariant state-space form. In order to account for unsteady aerodynamics, the aerodynamic forces have to be described as a rational function of the Laplace variable (s), as has been shown in various applications such as those of Sevart (ref. 1) and Edwards (ref. 2). Systematic techniques that use oscillatory aerodynamic matrices (defined along the imaginary axis of the s-plane) to generate rational approximate solutions for arbitrary motion were developed by several authors. The most widely used techniques are those based on the least-squares (LS) method of Roger (ref. 3) and the matrix-Padé (MP) method of Vepa (ref. 4). The resulting state-space equations include augmented states that represent the aerodynamic lags. The number of aerodynamic augmented states resulting from Roger's and Vepa's methods is equal to the number of the approximating denominator roots, multiplied by the number of vibration modes. Karpel (refs. 5 and 6) introduced the minimum-state (MS) method in which a higher number of denominator roots are required per given accuracy. However, the number of augmenting states resulting from this method is equal to the number of the denominator roots, regardless of the number of modes. The minimum-state approximation solution of references 5 and 6 implies perfect fit of the steady aerodynamics and of the aerodynamic matrix at one other reduced frequency value to be chosen by the analyst. A nonlinear, iterative least-squares method is used to approximate the other tabulated aerodynamic matrices.

Tiffany and Adams (refs. 7–9) extended the least-squares method, the modified matrix-Padé method, and the minimum-state method to include the capability for enforcing or relaxing various equality constraints as desired by the analyst. These extensions, abbreviated by ELS, EMMP, and EMS, respectively, are the optional approximation methods in the Interaction of Structures, Aerodynamics, and Controls (ISAC) computer program, which is an updated version of reference 10. The EMS method has no requirements on the number of constraints enforced. Although certain types of constraints are solved explicitly, other types are enforced by a Lagrangian multiplier technique that increases the number of simultaneous equations to be solved. Hence, the effect of the flexibility in constraint selection on the minimum-state method is to increase the number of equations solved simultaneously in each least-squares iteration step. This can slow down the iterative process and cause computational limitations to be reached sooner. Tiffany and Adams also employ nonlinear programming techniques to optimize the values of the approximation roots with respect to an overall error function. Their experience was that applying this optimization to the minimum-state method requires considerably more computation time than applying it to the other methods since it adds another iteration process to a method that already requires a two-step iteration process. On the other hand, since the minimum-state method allows a larger number of distinct approximation roots than allowed by the other methods, optimization is not as important. The various numerical examples of references 5, 6, 9, and 11 demonstrated that the MS method yields a significant reduction of the number of aerodynamic states (by a factor of 2 or more) relative to the other methods.

Karpel (ref. 11) modified the original minimum-state formulation to accept weighted data and to allow more constraint options without increasing the problem size. In calculating an overall error

function, Tiffany and Adams normalized the fit errors of each aerodynamic coefficient but treated the different tabulated points for each aerodynamic coefficient as equally important (except for the imposed equality constraint points). The physical weighting algorithm suggested in reference 11 weights different data terms according to the effect of their errors on aeroelastic characteristics. This weighting yields a better fit of the more important terms, at the expense of less important ones, and thereby increases the accuracy of the subsequent aeroservoelastic system behavior.

The formulation of reference 11 is the basis of the Minimum-State (MIST) computer program. The purpose of this paper is to outline and expand key equations in the way that they are used in the program to describe the program structure, main features, and interfaces with ISAC, and also to give a new numerical example, with a further investigation of the different options and emphasis on the physical weighting method.

2. Approximation Equations and Solution Procedures

2.1. Equations of Motion

The common approach for formulating the equations of motion of an aeroelastic system starts with a normal modes analysis of the structural system. A set of low-frequency normal vibration modes is chosen to represent the structural motion in generalized coordinates. Aeroservoelastic formulation requires additional modes to represent the control-surface commanded deflections. These modes are defined herein by a rigid rotation of a control surface and zero deflections elsewhere. Gust velocity modes can also be introduced if required. The complex, generalized, unsteady aerodynamic force coefficient matrix $[\mathbf{Q}(s)]$ is defined by the Laplace transform of its structural-, control-, and gust-related partitions, $[\mathbf{Q}_s(s)]$, $[\mathbf{Q}_c(s)]$, and $[\mathbf{Q}_g(s)]$, respectively, as

$$\{\mathbf{F}_s(s)\} = -q\,[\mathbf{Q}_s(s)]\,\{\boldsymbol{\xi}(s)\} - q\,[\mathbf{Q}_c(s)]\,\{\boldsymbol{\delta}_c(s)\} - \frac{q}{V}\,[\mathbf{Q}_g(s)]\,\{\mathbf{w}_g(s)\} \tag{1}$$

where $\{\mathbf{F}_s\}$ is the vector of n_s generalized aerodynamic forces on the vibration modes, $\{\boldsymbol{\xi}\}$ is the vector of n_s generalized structural displacements, $\{\mathbf{w}_g\}$ is the vector of n_g gust velocities, and $\{\boldsymbol{\delta}_c\}$ is the vector of n_c control-surface commanded deflections, namely, the actuator angular outputs. It is assumed in this work that control-surface hinge-moment effects are insignificant (i.e., the controls are irreversible) and, consequently, the control-related rows of $[\mathbf{Q}(s)]$ are eliminated. These terms are dealt with in reference 11.

The Laplace transform of the open-loop aeroelastic-system equations of motion, excited by control surface and gust input, can be written as

$$[\mathbf{C}(s)]\,\{\boldsymbol{\xi}(s)\} = -\left([\mathbf{M}_c]\,s^2 + q\,[\mathbf{Q}_c(s)]\right)\{\boldsymbol{\delta}_c(s)\} - \frac{q}{V}\,[\mathbf{Q}_g(s)]\,\{\mathbf{w}_g(s)\} \tag{2}$$

where

$$[\mathbf{C}(s)] = [\mathbf{M}_s]\,s^2 + [\mathbf{B}_s]\,s + [\mathbf{K}_s] + q\,[\mathbf{Q}_s(s)]$$

where $[\mathbf{M}_s]$, $[\mathbf{B}_s]$, and $[\mathbf{K}_s]$ are the generalized structural mass, damping, and stiffness matrices, respectively, and $[\mathbf{M}_c]$ is the coupling mass matrix between the control and the structural modes. In order to transform equation (2) into a time-domain, constant coefficient set of equations, the aerodynamic matrix $[\mathbf{Q}(s)]$ has to be described as a rational function of s. The minimum-state method used in references 6, 8, 9, and 11 approximates $[\mathbf{Q}(s)]$ by

$$\left[\widetilde{\mathbf{Q}}(p)\right] = [\mathbf{A}_0] + [\mathbf{A}_1]p + [\mathbf{A}_2]p^2 + [\mathbf{D}](p[\mathbf{I}] - [\mathbf{R}])^{-1}[\mathbf{E}]p \tag{3}$$

where

$$\left[\widetilde{\mathbf{Q}}(p)\right] \equiv \left[\widetilde{\mathbf{Q}}_s(p)\;\; \widetilde{\mathbf{Q}}_c(p)\;\; \widetilde{\mathbf{Q}}_g(p)\right]$$

and where p is the nondimensionalized Laplace variable given as $p = sb/V$. The real-valued approximation matrices of equation (3) are then partitioned as

$$\left.\begin{aligned} [\mathbf{A}_i] &= [\mathbf{A}_{s_i}\;\; \mathbf{A}_{c_i}\;\; \mathbf{A}_{g_i}] \qquad (i = 0, 1, 2) \\ [\mathbf{D}] &= [\mathbf{D}_s] \\ [\mathbf{E}] &= [\mathbf{E}_s\;\; \mathbf{E}_c\;\; \mathbf{E}_g] \end{aligned}\right\} \tag{4}$$

It is assumed herein that $[\mathbf{A}_{g_2}] = 0$. The resulting time-domain, state-space open-loop equation of motion is

$$\{\dot{\mathbf{x}}\} = [\mathbf{A}]\,\{\mathbf{x}\} + [\mathbf{B}]\,\{\mathbf{u}\} + [\mathbf{B}_w]\,\{\mathbf{w}\} \tag{5}$$

where

$$\left.\begin{aligned} \{\mathbf{x}\} &= \begin{Bmatrix} \xi \\ \dot{\xi} \\ \mathbf{x}_a \end{Bmatrix} \\ [\mathbf{A}] &= \begin{bmatrix} 0 & \mathbf{I} & 0 \\ -\overline{\mathbf{M}}_s^{-1}(\mathbf{K}_s + q\mathbf{A}_{s_0}) & -\overline{\mathbf{M}}_s^{-1}\left(\mathbf{B}_s + \frac{qb}{V}\mathbf{A}_{s_1}\right) & -q\overline{\mathbf{M}}_s^{-1}\mathbf{D} \\ 0 & \mathbf{E}_s & \frac{V}{b}\mathbf{R} \end{bmatrix} \end{aligned}\right\} \tag{6a}$$

$$\left.\begin{aligned} \{\mathbf{u}\} &= \begin{Bmatrix} \delta_c \\ \dot{\delta}_c \\ \ddot{\delta}_c \end{Bmatrix} \\ [\mathbf{B}] &= \begin{bmatrix} 0 & 0 & 0 \\ -q\overline{\mathbf{M}}_s^{-1}\mathbf{A}_{c_0} & -\frac{qb}{V}\overline{\mathbf{M}}_s^{-1}\mathbf{A}_{c_1} & -\overline{\mathbf{M}}_s^{-1}\left(\mathbf{M}_c + \frac{qb^2}{V^2}\mathbf{A}_{c_2}\right) \\ 0 & \mathbf{E}_c & 0 \end{bmatrix} \end{aligned}\right\} \tag{6b}$$

$$\left.\begin{aligned} \{\mathbf{w}\} &= \begin{Bmatrix} \mathbf{w}_g \\ \dot{\mathbf{w}}_g \end{Bmatrix} \\ [\mathbf{B}_w] &= \begin{bmatrix} 0 & 0 \\ -\frac{q}{V}\overline{\mathbf{M}}_s^{-1}\mathbf{A}_{g_0} & -\frac{qb}{V^2}\mathbf{A}_{g_1} \\ 0 & \mathbf{E}_g \end{bmatrix} \end{aligned}\right\} \tag{6c}$$

where

$$[\overline{\mathbf{M}}_s] = [\mathbf{M}_s] + \frac{qb^2}{V^2}[\mathbf{A}_{s_2}]$$

and where $\{\mathbf{x}_a\}$ is the vector of aerodynamic states. For closed-loop analysis, the states of equation (5) are augmented with control-system related states.

2.2. The Minimum-State Approximation Procedure

Tabular unsteady aerodynamic complex matrices calculated for several reduced frequency values ($k_\ell = \omega_\ell b/V$) along the imaginary axis of the nondimensional Laplace p-plane, namely, at various $p = ik_\ell$ points, are approximated with rational functions using the minimum-state approach. The full development of the minimum-state approach is given in reference 6. Key equations are repeated here. The equations for alternative constraint sets that incorporate some constraint selectability without adversely affecting the problem size along with the iterative process for determining the approximation are described herein. The real and imaginary parts of the aerodynamic approximation of equation (3) with $p = ik$ are

$$\left[\widetilde{\mathbf{F}}(k)\right] = [\mathbf{A}_0] - [\mathbf{A}_2]\,k^2 + k^2[\mathbf{D}]\left(k^2[\mathbf{I}] + [\mathbf{R}]^2\right)^{-1}[\mathbf{E}] \tag{7}$$

and

$$\left[\widetilde{\mathbf{G}}(k)\right] = [\mathbf{A}_1]\,k - k\,[\mathbf{D}]\left(k^2[\mathbf{I}] + [\mathbf{R}]^2\right)^{-1}[\mathbf{R}][\mathbf{E}] \tag{8}$$

For a given root matrix $[\mathbf{R}]$, the problem is to find the combination of $[\mathbf{A}_0]$, $[\mathbf{A}_1]$, $[\mathbf{A}_2]$, $[\mathbf{D}]$, and $[\mathbf{E}]$ that best fits the tabulated aerodynamic matrices

$$[\mathbf{Q}(ik_\ell)] = [\mathbf{F}(k_\ell)] + i[\mathbf{G}(k_\ell)]$$

where $[\mathbf{F}]$ and $[\mathbf{G}]$ are real matrices. Three approximation constraints are used to reduce the problem size by explicitly determining $[\mathbf{A}_0]$, $[\mathbf{A}_1]$, and $[\mathbf{A}_2]$ of equations (7) and (8). The constraints are given as follows:

1. A data-match constraint at $k = 0$, which yields

$$[\mathbf{A}_0] = [\mathbf{F}(0)] \tag{9}$$

2. Either a real-part data-match constraint at a nonzero $k = k_f$, that is,

$$[\widetilde{\mathbf{F}}(k_f)] = [\mathbf{F}(k_f)]$$

which, when using constraint 1, yields

$$[\mathbf{A}_2] = \left([\mathbf{F}(0)] - [\mathbf{F}(k_f)]\right) \Big/ k_f^2 + [\mathbf{D}] \left(k_f^2[\mathbf{I}] + [\mathbf{R}]^2\right)^{-1} [\mathbf{E}] \tag{10}$$

or an approximation constraint (which is always used for gust-related terms):

$$[\mathbf{A}_2] = [0] \tag{11}$$

The real-part approximation equations at the nonmatched tabulated k_ℓ values are

$$k_\ell^2[\mathbf{D}]\,[\overline{\mathbf{C}}_f(k_\ell)]\,[\mathbf{E}] \approx [\overline{\mathbf{F}}(k_\ell)] \tag{12}$$

where, when the real-part data-match constraint at $k = k_f$ is applied,

$$[\overline{\mathbf{C}}_f(k_\ell)] = \left(k_\ell^2[\mathbf{I}] + [\mathbf{R}]^2\right)^{-1} - \left(k_f^2[\mathbf{I}] + [\mathbf{R}]^2\right)^{-1} \tag{13a}$$

and

$$[\overline{\mathbf{F}}(k_\ell)] = ([\mathbf{F}(k_\ell)] - [\mathbf{F}(0)]) - ([\mathbf{F}(k_f)] - [\mathbf{F}(0)])\,\frac{k_\ell^2}{k_f^2} \tag{13b}$$

or, when the $[\mathbf{A}_2] = 0$ constraint is applied,

$$[\overline{\mathbf{C}}_f(k_\ell)] = \left(k_\ell^2[\mathbf{I}] + [\mathbf{R}]^2\right)^{-1} \tag{14a}$$

and

$$[\overline{\mathbf{F}}(k_\ell)] = [\mathbf{F}(k_\ell)] - [\mathbf{F}(0)] \tag{14b}$$

3. Either an imaginary-part data-match constraint at a nonzero $k = k_g$, which yields

$$[\mathbf{A}_1] = [\mathbf{G}(k_g)] \Big/ k_g + [\mathbf{D}] \left(k_g^2[\mathbf{I}] + [\mathbf{R}]^2\right)^{-1} [\mathbf{R}][\mathbf{E}] \tag{15}$$

or an approximation slope constraint:

$$[\mathbf{A}_1] = [0] \tag{16}$$

The imaginary-part approximation equations at the nonmatched tabulated k_ℓ values are

$$k_\ell[\mathbf{D}]\,[\overline{\mathbf{C}}_g(k_\ell)]\,[\mathbf{R}][\mathbf{E}] \approx [\overline{\mathbf{G}}(k_\ell)] \tag{17}$$

where, when the imaginary data-match constraint at $k = k_g$ is applied,

$$[\overline{\mathbf{C}}_g(k_\ell)] = \left(k_\ell^2[\mathbf{I}] + [\mathbf{R}]^2\right)^{-1} - \left(k_g^2[\mathbf{I}] + [\mathbf{R}]^2\right)^{-1} \tag{18a}$$

and

$$[\overline{\mathbf{G}}(k_\ell)] = [\mathbf{G}(k_g)]\,\frac{k_\ell}{k_g} - [\mathbf{G}(k_\ell)] \tag{18b}$$

or, when the $[\mathbf{A}_1] = 0$ constraint is applied,

$$[\overline{\mathbf{C}}_g(k_\ell)] = \left(k_\ell^2[\mathbf{I}] + [\mathbf{R}]^2\right)^{-1} \tag{19a}$$

and

$$[\overline{\mathbf{G}}(k_\ell)] = -[\mathbf{G}(k_\ell)] \tag{19b}$$

It should be noted that different constraints may be assigned to different aerodynamic terms, or even to the real and imaginary parts of the same term. A description of the constraint options in the MIST computer program is given in appendix A.

The $m \times m$ matrix $[\mathbf{R}]$ is diagonal with distinct negative terms. Default values are provided for initial estimates of the $n_s \times m$ $[\mathbf{D}]$ matrix which may be overridden by the analyst. The default choice is a zero matrix except for all diagonal elements $\mathbf{D}_{ii}$ and $\mathbf{D}_{(\nu m+i)i}$ (when $n_s > m$, where ν is an arbitrary positive integer) or $\mathbf{D}_{i(\nu n_s+i)}$ (when $m > n_s$) which are equal to 1. For a given $[\mathbf{R}]$ and an initial value of $[\mathbf{D}]$, equations (12) and (17) provide an overdetermined set of approximate equations for each column of $[\mathbf{E}]$. This set of equations can be solved by the least-squares approach in which each data term in the right-hand side of equations (12) and (17) may be assigned a weight $\mathbf{W}_{ij\ell}$, where the real and the imaginary parts are assigned the same set of weights. The weighted least-squares solution for the jth column of $[\mathbf{E}]$ is obtained by solving

$$\sum_\ell \left([\mathbf{A}_{f_\ell}]^T \left\lceil \mathbf{W}_{j\ell} \right\rfloor^2 [\mathbf{A}_{f_\ell}] + [\mathbf{A}_{g_\ell}]^T \left\lceil \mathbf{W}_{j\ell} \right\rfloor^2 [\mathbf{A}_{g_\ell}] \right) \{\mathbf{E}_j\} = \sum_\ell \left([\mathbf{A}_{f_\ell}]^T \left\lceil \mathbf{W}_{j\ell} \right\rfloor^2 \{\overline{\mathbf{F}}_j(k_\ell)\} + [\mathbf{A}_{g_\ell}]^T \left\lceil \mathbf{W}_{j\ell} \right\rfloor^2 \{\overline{\mathbf{G}}_j(k_\ell)\} \right) \tag{20}$$

where

$$\left[\mathbf{A}_{f_\ell}\right] = \left[k_\ell^2 \mathbf{D}\ \overline{\mathbf{C}}_f(k_\ell)\right] \tag{21a}$$

and

$$[\mathbf{A}_{g_\ell}] = [k_\ell \mathbf{D}\ \overline{\mathbf{C}}_g(k_\ell)\ \mathbf{R}] \tag{21b}$$

where $\left\lceil \mathbf{W}_{j\ell} \right\rfloor$ represents the diagonal elements of the matrix formed by taking the jth column from each weight matrix $[\mathbf{W}]_\ell$ assigned to $[\mathbf{Q}(ik_\ell)]$. Here, $\{\overline{\mathbf{F}}_j(k_\ell)\}$ and $\{\overline{\mathbf{G}}_j(k_\ell)\}$ are the jth columns of

$[\overline{\mathbf{F}}(k_\ell)]$ and $[\overline{\mathbf{G}}(k_\ell)]$ of equations (12) and (17), respectively.

After solving for [**E**], a least-squares solution is obtained for the rows of [**D**] by solving

$$\sum_\ell \left(\left[\mathbf{A}^*_{f_\ell}\right]^T \left[\mathbf{W}_{i\ell}\right]^2 \left[\mathbf{A}^*_{f_\ell}\right] + \left[\mathbf{A}^*_{g_\ell}\right]^T \left[\mathbf{W}_{i\ell}\right]^2 \left[\mathbf{A}_{g_\ell}\right] \right) \left\{\mathbf{D}_i^T\right\}$$

$$= \sum_\ell \left(\left[\mathbf{A}^*_{f_\ell}\right]^T \left[\mathbf{W}_{i\ell}\right]^2 \left\{\overline{\mathbf{F}}_i(k_\ell)\right\} + \left[\mathbf{A}^*_{g_\ell}\right]^T \left[\mathbf{W}_{i\ell}\right]^2 \left\{\overline{\mathbf{G}}_i(k_\ell)\right\} \right) \tag{22}$$

where

$$\left[\mathbf{A}^*_{f_\ell}\right] = \left[k_\ell^2 \mathbf{E}^T\, \overline{\mathbf{C}}_f(k_\ell)\right] \tag{23a}$$

and

$$\left[\mathbf{A}^*_{g_\ell}\right] = \left[k_\ell \mathbf{E}^T \mathbf{R}\, \overline{\mathbf{C}}_g(k_\ell)\right] \tag{23b}$$

where $\left[\mathbf{W}_{i\ell}\right]$ represents the diagonal elements of the matrix formed by taking the ith row from each $[\mathbf{W}]_\ell$, and $\left\{\overline{\mathbf{F}}_i(k_\ell)\right\}^T$ and $\left\{\overline{\mathbf{G}}_i(k_\ell)\right\}^T$ are the ith rows of $[\overline{\mathbf{F}}(k_\ell)]$ and $[\overline{\mathbf{G}}(k_\ell)]$, respectively. The procedure repeats alternate solutions for [**E**] and [**D**]. After each [**D**] $\rightarrow$ [**E**] $\rightarrow$ [**D**] cycle, the procedure calculates the overall error:

$$\epsilon_t = \sqrt{\sum_{ij\ell} \epsilon_{ij\ell}^2} \tag{24}$$

where

$$\epsilon_{ij\ell} = |\tilde{\mathbf{Q}}_{ij}(ik_\ell) - \mathbf{Q}_{ij}(ik_\ell)|\mathbf{W}_{ij\ell}$$

where $\mathbf{W}_{ij\ell}$ is the (i,j)th term of $[\mathbf{W}]_\ell$. The nonlinear iterative solution terminates after convergence is obtained for ϵ_t.

3. Data Weighting

3.1. Data Normalization

Tiffany and Adams (refs. 8 and 9) used a normalized total error function for evaluating an overall goodness of fit for all the aerodynamic approximations. This error function was employed to avoid mode normalization effects on the least-squares solution. If the weights in equation (24) are defined so that each

$$\mathbf{W}_{ij\ell} = \mathbf{W}^*_{ij} \tag{25}$$

where

$$\mathbf{W}^*_{ij} = \frac{1}{\max\limits_\ell \left(|\mathbf{Q}_{ij}(ik_\ell)|,\ 1\right)}$$

then the overall error function ϵ_t is equivalent to the weighted error function defined in reference 9, with unit weights therein. The absolute value of a weighted aerodynamic term is

$$\overline{\mathbf{Q}}_{ij}(k_\ell) = \mathbf{W}^*_{ij}|\mathbf{Q}_{ij}(ik_\ell)| \tag{26}$$

The effect of this weighting is renormalization of the input data such that the maximum $\overline{\mathbf{Q}}(k_\ell)$ of each (i,j)th term is 1, with the exception of terms with maximum $|\mathbf{Q}(ik_\ell)|$ of less than 1 which are not normalized. Thus, ϵ_t of equation (24) is consistent with the "common measure of approximation performance" of reference 9. The computer program MIST allows for this data normalization weighting in order to compare results with the ISAC program.

3.2. Physical Weighting

The physical weighting is designed to weight each term of the tabulated data according to a "measure of importance," which is based on the partial derivative of a selected open-loop characteristic parameter, at nominal flow conditions, with respect to the weighted term. Three groups of weights associated with $[\mathbf{Q}_s]$, $[\mathbf{Q}_c]$, and $[\mathbf{Q}_g]$ of equation (1) are defined. The resulting weight matrices $[\mathbf{W}]_\ell$ are a function of k_ℓ and, like the data normalization weights, they lead to least-squares solutions in which mode normalization effects are avoided.

3.2.1. Structural mode measure of importance. The weighting of a term $\mathbf{Q}_{s_{ij}}$ in the mode-related matrix $[\mathbf{Q}_s]$ is based on the derivative of the open-loop system determinant $\|\mathbf{C}(ik)\|$ of equation (2), with respect to that term:

$$\frac{\partial \|\mathbf{C}(ik)\|}{\partial \mathbf{Q}_{s_{ij}}} = -q \times \text{Cofactor}\left[\mathbf{C}_{ij}(k)\right] \tag{27}$$

The measure of importance associated with $\mathbf{Q}_{s_{ij}}(ik_\ell)$ is defined by the absolute value of this cofactor divided by $\|\mathbf{C}(ik)\|$, which is actually the absolute value of the (j,i)th term in $[\mathbf{C}(ik_\ell)]^{-1}$. The resulting structural measure-of-importance matrix is

$$\left[\overline{\mathbf{W}}_s\right]_\ell = \left|\left[\mathbf{C}(ik_\ell)\right]^{-1}\right|^T \tag{28}$$

3.2.2. Control mode measure of importance. The weights associated with the jth column of the control-surface related matrix $[\mathbf{Q}_c]$ are based on the open-loop output response of the jth actuator to sinusoidal excitation by the jth control surface

$$\delta_{c_j}(i\omega) = \{\mathbf{T}_j(i\omega)\}^T [\Psi_m] [\mathbf{C}(i\omega)]^{-1} \left(q \left\{ \mathbf{Q}_{c_j}(i\omega) \right\} + \omega^2 \left\{ \mathbf{M}_{c_j} \right\} \right) \quad (29)$$

where $[\Psi_m]$ is the matrix of modal deflections or rotations at the sensor input points, $\{\mathbf{Q}_{c_j}\}$ and $\{\mathbf{M}_{c_j}\}$ are the jth columns of $[\mathbf{Q}_c]$ and $[\mathbf{M}_c]$, respectively, of equation (2), and $\{\mathbf{T}_j(i\omega)\}^T$ is the jth row of the matrix of transfer functions from sensor inputs to actuator outputs chosen by the analyst to be included in the weighting scheme. These transfer functions should reflect basic characteristics of the control system such as measurement type, actuator dynamics, and the (nonzero) order of magnitude of the control gains. A high level of accuracy is not required, and narrowband control components such as high-order structural filters should not be included in order to avoid the assignment of low weights to aerodynamic terms which may be important in a subsequent control design process.

The frequency response of equation (29) is actually a Nyquist parameter that characterizes the aeroservoelastic loop associated with the jth control surface. The measure of importance of the $\mathbf{Q}_{c_{ij}}(ik_\ell)$ term is the absolute value of the derivative of δ_{c_j} with respect to $\mathbf{Q}_{c_{ij}}$, which yields the control measure-of-importance matrix:

$$[\overline{\mathbf{W}}_c]_\ell = q | [\mathbf{T}(ik_\ell)] [\Psi_m] [\mathbf{C}(ik_\ell)]^{-1} |^T \quad (30)$$

3.2.3. Gust mode measure of importance. The weighting of the gust-related matrix $[\mathbf{Q}_g]$ is based on the power spectral density (PSD) of the open-loop response of selected structural points to continuous gust with Dryden's PSD function. When the acceleration response is of interest, the PSD of the response associated with the jth gust column is

$$\Phi_{z_j}(\omega) = | \frac{\omega^2 q}{V} \{\Psi_{z_j}\}^T [\mathbf{C}(i\omega)]^{-1} \{\mathbf{Q}_{g_j}(i\omega)\} |^2 \Phi_{g_j}(\omega) \quad (31)$$

where $\{\Psi_{z_j}\}^T$ is the vector of modal deflections at a structural point that responds well to the jth gust, $\{\mathbf{Q}_{g_j}\}$ is the jth column of $[\mathbf{Q}_g]$, and $\Phi_{g_j}(\omega)$ is Dryden's PSD function:

$$\Phi_{g_j} = \frac{\sigma_{g_j}^2}{\pi} \frac{L_g}{V} \frac{1 + 3(k_\ell L_g/b)^2}{[1 + (k_\ell L_g/b)^2]^2} \quad (32)$$

where σ_{g_j} is the jth gust root-mean-square (rms) velocity, and L_g is the gust characteristic length.

The measure of importance of $Q_{g_{ij}}$ is the derivative of $\sqrt{\Phi_{z_j}(\omega)}$ with respect to $Q_{g_{ij}}$, which yields the following gust measure-of-importance matrix:

$$[\overline{\mathbf{W}}_g]_\ell = \frac{k_\ell^2 q V}{b^2} | [\Psi_z] [\mathbf{C}(ik_\ell)]^{-1} |^T \left[\sqrt{\Phi_g(k_\ell)} \right] \quad (33)$$

Thus, we have the measure-of-importance matrix

$$[\mathbf{W}]_\ell = [\overline{\mathbf{W}}_{ij\ell}] = [[\overline{\mathbf{W}}_s]_\ell \quad [\overline{\mathbf{W}}_c]_\ell \quad [\overline{\mathbf{W}}_g]_\ell]$$

3.2.4. Physical weights. The weight matrices of each group are obtained by separately normalizing the measure-of-importance matrices such that the maximum absolute value of the weighted tabulated terms in each group is 1. The absolute value of each tabulated aerodynamic term is first multiplied by its measure-of-importance value. The maximum resulting values (for each term separately) are

$$\widetilde{\mathbf{W}}_{ij} = \max_\ell [|\mathbf{Q}_{ij}(ik_\ell)| \overline{\mathbf{W}}_{ij\ell}] \quad (34)$$

The weights of each group can now be defined. The mode-related weight matrix $[\mathbf{W}_s]_\ell$ has elements defined by

$$(\mathbf{W}_s)_{ij\ell} = (\overline{\mathbf{W}}_s)_{ij\ell} \left(\max \left\{ \frac{1}{\max_{i,j} \left[\left(\widetilde{\mathbf{W}}_s \right)_{ij} \right]}, \frac{w_{\text{cut}}}{(\widetilde{\mathbf{W}}_s)_{ij}} \right\} \right) \quad (35)$$

where w_{cut} is a user-defined minimum weight limit. The other group weight matrices $[\mathbf{W}_c]_\ell$ and $[\mathbf{W}_g]_\ell$ are defined similarly. Thus, the physical weight matrix is defined as follows:

$$[\mathbf{W}]_\ell = [\mathbf{W}_{ij\ell}] = [[\mathbf{W}_s]_\ell \quad [\mathbf{W_c}]_\ell \quad [\mathbf{W}_g]_\ell]$$

Note that the maximum weighted aerodynamic value of each aerodynamic term is

$$\mathbf{Q}_{ij}^* = \max_\ell \left[\overline{\mathbf{Q}}_{ij}(k_\ell) \right] \quad (36)$$

where

$$\overline{\mathbf{Q}}_{ij}(k_\ell) = \mathbf{W}_{ij\ell} |\mathbf{Q}_{ij}(ik_\ell)|$$

falls between a user-defined w_{cut} value and 1.0.

As will be demonstrated in section 4.2.1., typical variations of weighted aerodynamic magnitudes versus k exhibit sharp peaks at tabulated reduced frequencies of particular importance. To assure good results at k values that fall between the tabulated ones and to facilitate the application of the resulting aeroelastic model to a variety of flow conditions

and control effects, it may be desired to widen the range of high weights. Consequently, the weighting procedure has been modified to allow the user to perform n_{wd} weight-peak widening cycles where, in each cycle, each measure-of-importance value $\overline{\mathbf{W}}_{ij\ell}$ is set to be equal to max $\left(\overline{\mathbf{W}}_{ij(\ell-1)},\ \overline{\mathbf{W}}_{ij\ell},\ \overline{\mathbf{W}}_{ij(\ell+1)}\right)$ of the previous cycle. It may be noticed that with $w_{\text{cut}} = 0$ and $n_{wd} = 0$, the physical weights of this work are equal to those of reference 11. With $w_{\text{cut}} = 1.0$ and $n_{wd} = n_k - 2$, all the physical weighting effects are diminished and the weighting values are equal to those of the data normalization weighting.

4. Numerical Application to the Active Flexible Wing Model

The example herein is a numerical application to the wind-tunnel model of Rockwell's Active Flexible Wing (AFW) tested in the Langley Transonic Dynamics Tunnel. A top view of the aerodynamic model is given in figure 1. The circles indicate points at which modal data were obtained from the vibration analysis. The mathematical model consists of 16 antisymmetric modes: 1 rigid-body (roll) mode, 10 elastic modes, 4 control-surface deflection modes, and 1 gust mode. The doublet lattice generalized aerodynamic matrices at a Mach number of 0.9 are tabulated at 14 k values of 0, 0.005, 0.01, 0.05, 0.1, 0.2, 0.3, 0.4, 0.5, 0.6, 0.8, 1.0, 1.5, and 2.0. The control surfaces of figure 1 are driven by third-order actuators. The control system takes a single roll-rate measurement and commands the actuators via zero-order control gains $\mathbf{G}_i$ that were designed to yield adequate roll-rate performance.

Minimum-state (MS) approximations were calculated using the MIST computer program described in appendix B. The MS approximation cases are symbolized by mN or mP where m is the number of approximation roots, N denotes the normalization weighting of equation (25), and P denotes the physical weighting of equation (31). The approximation roots in all the analyzed MS cases, given in table 1, were arbitrarily spaced between the values of -0.03 and -3.1 and were not optimized.

4.1. Data Normalization Cases

4.1.1. The iterative approximation solution. The data normalization (N) cases are considered first. The initial 11×2 [**D**] matrix in the 2N case is the default one, namely, all zeros except for the $\mathbf{D}_{ii}$ and the $\mathbf{D}_{(2\ell+i)i}$ (with $\ell = 1$ to 5) terms which are equal to 1.0. The initial [**D**] in each subsequent case (with $m = 4, 6, 8$, etc.) is the final [**D**] of the previous case, expanded by default columns. The approximation constraints are data matched at $k = 0$ and $k_f = k_g = 2.0$. Here, 100 [**D**] $\rightarrow$ [**E**] $\rightarrow$ [**D**] iterations were performed in the 2N to 10N cases, and 50 iterations were performed in the 12N to 20N cases. Actual convergence is not tested in the program. The variations of the total approximation error ϵ_t with the number of iterations are given in figure 2. It can be observed that the errors are decreasing with the number of iterations, but the convergence rate may be nonmonotonic and slow. However, in all the analyzed cases the errors after 10 iterations are fairly close to the final ones.

4.1.2. Comparison with other approximation methods. The final total approximation errors of the MS N cases (data normalization) are given in table 2 and are compared in figure 3 with those obtained by the extended least-squares (ELS) method of Roger, as outlined in references 8 and 9. The ELS approximations were constrained to match the data at $k = 0$ only, and the approximation roots were optimized for best overall fit using ISAC. It can be observed that the MS method without physical weighting yields a similar total approximation error with less than 30 percent of the augmenting states resulting from the ELS method, even without optimization of the MS approximation roots.

4.2. Physical Weighting Cases

4.2.1. The physically weighted aerodynamic data. The physical weighting of the tabulated aerodynamic data was performed at a true flow velocity of $V = 5508$ in/sec and a dynamic pressure of $q = 1.5$ psi. The control gains G_i are 0.001, -1.0, 1.0, and -1.0; the gust length is $L_g = 1200$ in.; and the gust response parameter is acceleration at the wingtip. The weights were first calculated using equation (31) with $w_{\text{cut}} = 0$; namely, there is no low limit to the maximum weighted magnitudes of the tabulated aerodynamic terms $\mathbf{Q}^*_{ij}$. The probability density functions $P(0, \mathbf{Q}^*)$ of the resulting $\mathbf{Q}^*_{ij}$ values, namely, the fraction of aerodynamic terms whose weighted maximum values do not exceed $\mathbf{Q}^*$, are shown in figure 4 for each weighting group separately. It can be observed that only about 20 percent of the terms have $\mathbf{Q}^* > 0.1$ and that about 20 percent of the terms that are not aeroelastically active have $\mathbf{Q}^* < 10^{-3}$. In comparison, with data normalization all the terms have $\mathbf{Q}^*$ values of 1.0.

Variations of weighted aerodynamic magnitudes $\overline{\mathbf{Q}}$ of equation (26) with tabulated k values are shown in figure 5 for some highly weighted terms. Weighted aerodynamic terms of structural modes have peak

values around the natural frequencies of the associated modes. The weighted values of terms $(1, 13)$ and $(3, 15)$ are typical of control terms that have important effects on static aeroelastic or higher frequency phenomena. The weighting procedure can be used for other purposes such as mode selection for aeroelastic analysis and for investigation of flutter mechanisms.

4.2.2. Approximation convergence. MS approximations with the physically weighted data (P cases) were performed for the 2 to 10 root cases listed in table 1. Appendix C defines the program input and output required to execute one of these cases. Two methods were used to define the initial [**D**] matrices. The first method ($n = 1$) used the final [**D**] matrices of the corresponding N cases. The second method ($n = 2$) was the one described above for the N cases. The P cases are symbolized by $(m\text{P}, n - w_{\text{cut}})$. All the P approximations were calculated with 30 [**D**] $\rightarrow$ [**E**] $\rightarrow$ [**D**] iterations. The final physically weighted total approximation errors ϵ_t and the errors calculated with the normalization weighting of the N cases $\epsilon_{t_{\text{N}}}$ are given in table 2. The $\epsilon_{t_{\text{N}}}$ values of the P cases are always larger than those of the N cases. Values of $w_{\text{cut}} > 0$ yield higher ϵ_t values than those of $w_{\text{cut}} = 0$, but lower $\epsilon_{t_{\text{N}}}$ values. It can also be observed that the differences between the two methods of selecting the initial [**D**] matrix are small. Variations of total weighted approximation errors with the number of iterations for four P cases with $w_{\text{cut}} = 0$ and for one P case with $w_{\text{cut}} = 0.1$ are shown in figure 6. It can be observed that there are numerical difficulties in the (10P, 1–0) case with $w_{\text{cut}} = 0$. This happens because the low weights assigned to many terms effectively reduce the amount of data, which causes ill-conditioning in the matrices to be inverted in the 10th-order least-squares fit. With $w_{\text{cut}} = 0.1$, this difficulty disappears. The results of the (10P, 1–0) cases shown in table 2 are those obtained after five iterations, before the numerical difficulties start.

4.2.3. Approximation curve fit. Approximation curve fits for the structural vibration mode term $(5, 5)$, the control mode term $(3, 15)$, and the gust mode term $(1, 16)$ of the generalized aerodynamic force (GAF) matrix resulting from the 4N and the (4P, 1–0) cases are shown in the real-imaginary plane in figures 7(a), 7(b), and 7(c), respectively. These terms were selected from the relatively highly weighted terms of figure 5. The P case yields a better fit than the N case in the area of high weights: $k = 0.2$ to 0.5 for GAF$(5, 5)$, $k = 0$ to 0.4 for GAF$(3, 15)$, and $k = 0$ to 0.5 for GAF$(1, 16)$ as can be observed in figure 5. Some high-order approximation fits are shown in figure 8 for GAF$(4, 4)$. It can be observed that the curves are wiggly in the low-frequency region, which may cause numerical problems of the kind shown in figure 6 or introduce some inaccuracies in the resulting aeroelastic characteristics, as discussed below.

4.2.4. Accuracy of subsequent aeroelastic characteristics. The real test of the physical weighting is in the resulting aeroservoelastic characteristics. First- and second-order, open- and closed-loop root-loci calculations were performed with constant velocity and Mach number and varying dynamic pressure. The second-order calculations were performed using the STABCAR (ref. 12) module of ISAC in order to form baselines for evaluation of the first-order results that used the MS rational approximation for the aerodynamic data. In the "baseline" cases, ISAC employed the p-k method to calculate p-plane roots using quadratic interpolation of the same tabulated aerodynamic data as used by the first-order calculations. The first-order root-loci calculations were performed using the First-Order Aeroservoelastic Roots (FASER) computer program with the MS approximation results. The baseline flutter dynamic pressure and frequency, namely, the parameters at which a root-loci branch crosses the imaginary axis, are $q_f = 1.9474$ psi and $\omega_f = 87.423$ rad/sec ($k = 0.314$) for the open-loop case and $q_f = 1.3515$ psi and $\omega_f = 90.737$ rad/sec ($k = 0.321$) for the closed-loop case. The physical weights were calculated for $q = 1.5$ psi between these two. The q_f and ω_f percentage errors for the various MS cases are given in figure 9. In the low-order approximation range ($m < 5$), the physical weighting with $w_{\text{cut}} = 0$ improves the accuracy of flutter parameters significantly. Even though there is no need to upscale the low weights, the $w_{\text{cut}} = 0.1$ cases still yield a significant improvement relative to the N cases. In the intermediate range ($5 < m < 9$), the approximation order starts to be too high and the flutter percentage error level ceases to decrease, first in the (mP, 1–0) cases (at $m = 6$) and then in the N cases. The use of $w_{\text{cut}} = 0.1$ yields smoother error curves and reduces the P case error level to less than one-half that of the N cases. Consequently, there is no advantage in using an approximation order of $m > 9$ in the analyzed case. It should be noticed that the flutter dynamic pressures are off by -10 percent (closed-loop) and 30 percent (open-loop) from the nominal $q = 1.5$ psi for which the weights were calculated. This indicates that the physical weighting, calculated at one set of flow parameters, has a beneficial effect over a wide parameter range.

It may be concluded from the data given above that the parameter range for selecting the desired combination of accuracy and model size is between

$m = 2$ ($w_{\text{cut}} = 0$) and $m = 6$ ($w_{\text{cut}} = 0.1$), both of which yield flutter accuracy levels of 0.7 to 0.3 percent. A comparison between the structural root loci obtained by closed-loop, first-order analysis using the (4P, 1–0.07) approximation case with $w_{\text{cut}} = 0.07$ and those obtained by second-order analysis with the tabulated data is shown in figure 10. The first-order aerodynamic and actuator roots are beyond the plot limits. The differences between the two root loci are very small, and it may be concluded that this minimum-state approximation yields an adequate model for aeroservoelastic analysis.

4.2.5. Various approximation constraints. The case of (4P, 1) with $w_{\text{cut}} = 0.07$ is used to demonstrate the various constraint options of MIST. The resulting approximation errors ϵ_t and ϵ_{t_N} as well as the subsequent closed-loop flutter results are given in table 3. (In the discussion that follows, NKF is a user-input parameter that indicates to the program the type of constraints to be enforced. See appendix A and table 4.) The first four cases are given as follows: (1) data-match constraints as above at $k = 2.0$ (NKF = 14); (2) data-match constraints at $k = 0.3$ (NKF = 7); (3) data-match constraints of $\partial[\mathbf{Q}]/\partial k$ at $k = 0$ and the real part of $[\mathbf{Q}]$ at $k = 2.0$ (NKF = 0); and (4) data-match constraints of $\partial[\mathbf{Q}]/\partial k$ at $k = 0$ and an approximation constraint of $[\mathbf{A}_2] = 0$ (NKF = −2). All these cases yield flutter errors of less than 0.4 percent. The NKF = 7 case (which requires previous knowledge of the flutter reduced frequency) yields the lowest errors. The last case has the $[\mathbf{A}_2] = 0$ constraint of case 4, but the data-match requirement of $\partial[\mathbf{Q}]/\partial k$ at $k = 0$ has been replaced by the approximation constraint of $\mathbf{A}_1 = 0$ for the terms associated with the highest residualized (IRED) vibration modes and the associated gust terms. (See details in appendix A.) This constraint facilitates dynamic residualization which is beyond the scope of this work.

4.2.6. Calculation time comparisons. The elapsed time of the MIST run for the (4P, 1−0.7) case was 100 sec for the data weighting and 210 sec for the 30 $[\mathbf{D}]\rightarrow[\mathbf{E}]\rightarrow[\mathbf{D}]$ iterations on the VAX microcomputer. The first-order root-loci calculations with FASER took approximately 80 sec. In comparison, the "baseline," second-order, determinant-iteration root-loci calculations with STABCAR took 2950 sec (approximately 10 to 15 times longer). Hence, once an adequate minimum-state model is determined, all subsequent flutter analyses can be performed much faster using first-order methods rather than second-order methods.

5. Concluding Remarks

The minimum-state method for rational approximation of unsteady aerodynamic force coefficients has been modified to allow more combinations of constraints and supplemented with two data-handling algorithms, one for normalization and the other for physical weighting of the tabulated aerodynamic coefficients. The method yields an adequate first-order, linear, aeroservoelastic mathematical model in which the number of aerodynamic augmented states may be lower by 70 percent (with data normalization) to 90 percent (with physical weighting) than that required by other commonly used approximation methods. Aeroservoelastic models with flutter boundary error levels of less than 1 percent were obtained with only 4 to 6 aerodynamic states added to the 22 structural, 12 actuator, and 2 gust-spectrum-related states. In this range of approximation roots, the physically weighted solution is not very sensitive to the method of selecting the initial matrix $[\mathbf{D}]$ in the minimum-state iteration process and converges in less than 10 steps. The various constraint options yield similar levels of accuracy, with the exception of the $\mathbf{A}_1 = 0$ slope constraint, which should be avoided or used with caution.

The formulation in this work is the basis of the Minimum-State (MIST) computer program presented in an appendix. The approximation formula, the data normalization option, and the algorithm for iterative solution with a given set of approximation roots are similar to those of the extended minimum-state (EMS) option in the Interaction of Structures, Aerodynamics, and Controls (ISAC) system of programs. In computing and using the minimum-state approximations, the main differences between the two programs are as follows:

1. MIST requires exactly three approximation constraints. ISAC allows greater flexibility in the number and type of approximation constraints. Although MIST uses all the constraints to reduce the size of the approximation problem, ISAC only uses some constraints (when they are applied) to reduce the problem size. Some data-match constraints in ISAC increase the problem size. For example, the numerical application of this paper with four approximation roots requires an inversion of 4×4 matrices in each minimum-state iteration process. Using ISAC with no constraints would require the inversion of 37×37 matrices in the first part and 52×52 matrices in the second part of the minimum-state iteration process.

2. ISAC allows optimization of the root values (with a large computation time penalty as indicated

in NASA TP-2776 for the minimum-state case), but MIST does not.

3. MIST features an automated physical weighting procedure, but ISAC does not.

4. Even though the EMS option in ISAC is an integral part of a large computational system with many other analysis options, MIST is a small stand-alone program that uses two standard matrix-inversion library subroutines and can be easily adapted for interaction with any aeroelastic computational system.

NASA Langley Research Center
Hampton, VA 23665-5225
August 16, 1990

Appendix A

Application of Constraints in MIST

One of the major differences between MIST and the minimum-state option in ISAC is that the MIST approximation procedure requires three constraints (for each aerodynamic term). These constraints, two for the real parts and one for the imaginary parts, allow the elimination of the $[\mathbf{A}_0]$, $[\mathbf{A}_1]$, and $[\mathbf{A}_2]$ matrices of equations (7) and (8) from the nonlinear least-squares iterative solution of equations (12) and (17). Application of ISAC's methodology, which allows fewer constraints and yields a lower total approximation error, results in a much larger set of equations to be solved in each iteration. Since some constraints are usually desired, and use of the end-point constraints option discussed below usually results in small effects on the total approximation error, a large time benefit can be achieved by using constraints to reduce the number of equations in the iterative solution without a significant adverse effect on the approximation. However, sensitivity of the results to different constraints should be explored before determination of constraint selection is finalized.

In MIST, the steady aerodynamics ($k = 0$) data-match constraint (eq. (9)) is always applied. The two other constraints are either defined by the user-input parameter NKF or set by the program in the special cases that are discussed below. NKF identifies the tabulated reduced frequencies k_f and k_g at which the real and imaginary parts of the aerodynamic data are matched, respectively. The NKF options are as follows:

1. NKF $= 1$: $k_f = k_g = \max(k_\ell)$. This "end-point" constraint option usually yields the lowest total approximation error and should be used as a default.
2. NKF > 1: k_f and k_g are equal to the (NKF)th tabulated k. This option is to be used to achieve good accuracy around this k value. Low values of k_f may cause a wiggly approximation in the low-frequency region because of the nearness of the $k = 0$ constraint.
3. NKF $= 0$: $k_f = \max(k_\ell); k_g = k_2$. This imaginary-part constraint is equivalent to constraining $\partial\widetilde{\mathbf{Q}}/\partial(ik)$ at $k = 0$ to match that of the tabulated data (assuming that $k_2 \to 0$). This may be used to obtain accurate aerodynamic coefficients associated with rigid-body velocities.
4. NKF < 0: $[\mathbf{A}_2] = 0$. There is no real-part match constraint (other than at $k = 0$); and k_g is equal to the $(-\text{NKF})$th tabulated k. With this option there are no "aerodynamic mass" terms in $\overline{\mathbf{M}}_s$ of equation (6). This may be an advantage in a subsequent analysis as $\overline{\mathbf{M}}_s$ would not have to be repeatedly inverted for every q value.

There are two cases in which the MIST program sets constraints to some terms, ignoring those selected with NKF. These cases are defined by the input parameters NSKIP and IRED as in the following:

1. NSKIP < 0: The last NG $= -$NSKIP columns are related to gust modes. The user-set real-part constraint is replaced (for these columns only) by $[\mathbf{A}_2] = 0$. This enables the gust column of equations (5) and (6) to appear without the $\ddot{w}_g$ term.
2. IRED > 0: Assuming that the last IRED vibration modes are candidates for dynamic reduction in a subsequent program, in order to facilitate the dynamic reduction, data-match constraints are automatically replaced in some terms by approximation constraints. These approximation constraints and the associated partitions of the aerodynamic matrix are

$$\left[\begin{array}{c:c:c:c} \mathbf{Q}_{ss} & \mathbf{Q}_{sr} & \mathbf{Q}_{sc} & \mathbf{Q}_{sg} \\ (\,-\,) & ([\mathbf{A}_2] = 0) & (\,-\,) & ([\mathbf{A}_2] = 0) \\ \cdots & \cdots & \cdots & \cdots \\ \mathbf{Q}_{rs} & \mathbf{Q}_{rr} & \mathbf{Q}_{rc} & \mathbf{Q}_{rg} \\ ([\mathbf{A}_2] = 0) & ([\mathbf{A}_1] = [\mathbf{A}_2] = 0) & ([\mathbf{A}_2] = 0) & ([\mathbf{A}_1] = [\mathbf{A}_2] = 0) \end{array}\right]$$

where the subscripts s, r, c, and g are related to the retained structural modes, the reduction candidates, the control modes, and the gust modes, respectively.

Appendix B

The MIST Computer Program

B.1. Program Description

MIST is a FORTRAN-77 computer program. The program reads five input files, creates five output files, and writes information to a system output file that is normally assigned to the user terminal or automatically sent to a printer. A schematic of the program input and output files is given in figure 11.

Even though MIST can be used as a stand-alone program, it is designed to interact with ISAC through its input and output files. Most input data parameters can be extracted from ISAC's data complex (TAPE9) using the Data Complex Manager (DCM) module. Three output files are for a subsequent analysis by ISAC's modules. These files are **SPLANE.DAT** to be used as TAPE5 input to the SPLFIT module which plots the approximation curves, **SPLCOF.DAT** to be used as TAPE5 input to the DCM module for storing the approximation coefficients on the data complex (for subsequent state-space analysis by the DYNARES module), and **T5STAB_INT.DAT** to be used as a TAPE5 input to the STABCAR module for second-order analysis.

MIST is constructed of a main part, four built-in subroutines, and two library subroutines. A brief flowchart of the main part and the built-in subroutines is given in figure 12. The functions of the built-in subroutines are as follows:

Subroutine REAR: Reads the tabulated reduced frequency values and the associated aerodynamic matrices.

Subroutine DED: Performs a single [**D**]→[**E**]→[**D**] iteration and calculates the current approximation errors.

Subroutine WEIGHTS: Calculates weights to be applied in the least-squares solutions.

Subroutine TRANS: Calculates the control-system transfer function for physically weighting the control mode aerodynamics.

The library subroutines are as follows:

Subroutine DMTINV: Solves a real-coefficient system of equations via matrix inversion (double precision).

Subroutine DCXINV: Inverts a complex matrix (double precision).

B.2. Input Files

Up to five free-format data input files (indicated in fig. 11) may be required for executing a MIST run. A general description of the files, the conditions in which they are required, and the input aids are given below. Detailed descriptions of the input parameters and their limits are given in tables 1–5. The input files are as follows:

1. **IMIST.DAT** (file 1): User-input run parameters and restart data. This file is either constructed by the user for initiating an approximation case or constructed by a previous MIST run (as the **IM.DAT** output file) for restarting the [**D**]→[**E**]→[**D**] iterations with the last calculated [**D**] and /or weighting matrices. Before restarting, **IM.DAT** must be renamed as **IMIST.DAT**. A detailed description is given in table 4.
2. **TABF.DAT** (file 4): Flow and structural properties. This file is required for the physical weighting only (IWE = 2). The file may be first constructed by retrieving the natural frequencies (FREQ), the generalized masses (GMASS), and the structural dampings (DAMPINGS) from ISAC's data complex (TAPE9) using the DCM module. The first line is then replaced by

a record containing the weighting flow parameters. If the data contain gust columns, weighting gust parameters are added at the bottom of the file. A detailed file description is given in table 5.

3. **TABAERO.DAT** (file 5): Tabulated aerodynamic matrices (always required). This file may be constructed by retrieving the aerodynamic matrices (AERO) from ISAC's TAPE9 data complex using the DCM module. A detailed file description is given in table 6.

4. **TRAN.DAT** (file 6): Control system data. This file is required by subroutine TRANS for physical weighting only (IWE = 2), when the data contain control columns. This subroutine assumes roll-rate sensors, constant-gain control laws, and third-order actuators. A detailed file description is given in table 7.

5. **T5STAB_TAB.DAT**: STABCAR input (TAPE5) with tabulated matrices. This file is required only when the user intends to run STABCAR for a second-order analysis. MIST replaces the tabulated aerodynamic data with approximated aerodynamics (if ISTAB≠0). The file can be constructed by retrieving the AERO, GMASS, FREQ, DAMPINGS, and SENDEF (when required) from ISAC's TAPE9 using the DCM module. A detailed file description is given in table 8.

B.3. Output Files

A default-system output file and up to five additional output files (indicated in fig. 11) are produced by MIST. A description of the output files and their subsequent usage is given as follows:

1. Default-system output file: Run-time monitor parameters, described in table 9. Data written to this file are generally sent to user console. If running **BATCH**, this file is generally printed automatically at end of execution.

2. **IM.DAT** (file 2): Enables restarting the [**D**]→[**E**]→[**D**] iterations by renaming **IM.DAT** as **IMIST.DAT**. The parameters are described in table 4. The values of [**D**] (record 3) are the result of the last [**D**]→[**E**]→[**D**] iteration. IWE (record 1) is set to 1, which causes the restart run to read the previously calculated weights from **IMIST.DAT**.

3. **SPLANE.DAT** (file 3): The approximation coefficient matrices. These can be defined as TAPE5 for a subsequent SPLFIT run which plots the approximation curves. Created only if IFILE≠0. A detailed description is given in table 10.

4. **RES.DAT** (file 7): Echo of run parameters, iteration errors, and main results. A detailed description is given in table 11.

5. **T5STAB_INT.DAT** (file 9): STABCAR input file (TAPE5). This file is identical to **T5STAB_TAB.DAT** (table 8) except for the tabulated aerodynamic matrices (record 2) which are replaced by approximated ones. Created only if ISTAB≠0.

6. **SPLCOF.DAT** (file 10): The approximation coefficient matrices. To be used as TAPE5 for storing the data on ISAC's data complex (TAPE9) using the DCM module STORE command. The data are stored with code name SPLANE which consists of one record with NLAST words. NLAST is written by MIST to the system output file (user console, see table 12). Created only if IFILE≠0.

Appendix C

Input and Output for a Sample Run

Input files and the user-console printout for case (4P, 1–0.1) of section 4.2.2. are given in this appendix. The sample case is a four-root physically weighted approximation where the initial [**D**] is the final one of the corresponding data normalization case (4N) and where $w_{\text{cut}} = 0.1$. A block diagram of the MIST input and output files is given in figure 11. The input files **IMIST.DAT**, **TRAN.DAT**, and **TABF.DAT** are given in tables 13, 14, and 15, respectively. The printout to the user console is given in table 16.

References

1. Sevart, Francis D.: *Development of Active Flutter Suppression Wind Tunnel Testing Technology.* AFFDL-TR-74-126, U.S. Air Force, Jan. 1975. (Available from DTIC as AD B002 840L.)
2. Edwards, John William: *Unsteady Aerodynamic Modeling and Active Aeroelastic Control.* SUDAAR 504 (Grant NGL-05-020-007), Guidance & Control Lab., Stanford Univ., Feb. 1977. (Available as NASA CR-148019.)
3. Roger, Kenneth L.: Airplane Math Modeling Methods for Active Control Design. *Structural Aspects of Active Controls,* AGARD-CP-228, Aug. 1977, pp. 4-1–4-11.
4. Vepa, Ranjan: *Finite State Modeling of Aeroelastic Systems.* NASA CR-2779, 1977.
5. Karpel, Mordechay: Design for Active Flutter Suppression and Gust Alleviation Using State-Space Aeroelastic Modeling. *A Collection of Technical Papers—AIAA/ASME/ASCE/AHS 21st Structures, Structural Dynamics & Materials Conference, Part 2, May 1980,* pp. 604–611. (Available as AIAA-80-0766.)
6. Karpel, Mordechay: *Design for Active and Passive Flutter Suppression and Gust Alleviation.* NASA CR-3482, 1981.
7. Tiffany, Sherwood H.; and Adams, William M., Jr.: *Fitting Aerodynamic Forces in the Laplace Domain: An Application of a Nonlinear Nongradient Technique to Multilevel Constrained Optimization.* NASA TM-86317, 1984.
8. Tiffany, Sherwood H.; and Adams, William M., Jr.: Nonlinear Programming Extensions to Rational Function Approximations of Unsteady Aerodynamics. *A Collection of Technical Papers—AIAA/ASME/ASCE/AHS 28th Structures, Structural Dynamics and Materials Conference and AIAA Dynamics Specialists Conference, Part 2A,* Apr., 1987, pp. 406–420. (Available as AIAA-87-0854.)
9. Tiffany, Sherwood H.; and Adams, William M., Jr.: *Nonlinear Programming Extensions to Rational Function Approximation Methods for Unsteady Aerodynamic Forces.* NASA TP-2776, 1988.
10. Peele, Ellwood L.; and Adams, William M., Jr.: *A Digital Program for Calculating the Interaction Between Flexible Structures, Unsteady Aerodynamics and Active Controls.* NASA TM-80040, 1979.
11. Karpel, Mordechay: Time-Domain Aeroservoelastic Modeling Using Weighted Unsteady Aerodynamic Forces. *J. Guid., Control, & Dyn.,* vol. 13, no. 1, Jan.–Feb. 1990, pp. 30 37.
12. Adams, William M., Jr.; Tiffany, Sherwood H.; Newsom, Jerry R.; and Peele, Ellwood L.: *STABCAR—A Program for Finding Characteristic Roots of Systems Having Transcendental Stability Matrices.* NASA TP-2165, 1984.

Symbols

$\mathbf{A}$	$(2n_s + m) \times (2n_s + m)$ open-loop state-form system matrix (eq. (5))
$\mathbf{A}_{f_\ell}, \mathbf{A}_{g_\ell}$	weighted least-squares matrices defined in equation (21)
$\mathbf{A}^*_{f_\ell}, \mathbf{A}^*_{g_\ell}$	weighted least-squares matrices defined in equation (23)
$\mathbf{A}_0, \mathbf{A}_1, \mathbf{A}_2$	$n_s \times (n_s + n_c + n_g)$ coefficient matrices of rational approximation (eq. (3))
$\mathbf{B}$	$(2n_s + m) \times 3n_c$ state-form control matrix (eq. (5))
$\mathbf{B}_s$	$n_s \times n_s$ generalized structural damping matrix
$\mathbf{B}_w$	$(2n_s + m) \times 2n_g$ state-form control matrix (eq. (5))
b	reference semichord
$\mathbf{C}$	$n_s \times n_s$ open-loop system matrix (eq. (2))
$\overline{\mathbf{C}}_f$	defined in equations (13a) or (14a)
$\overline{\mathbf{C}}_g$	defined in equations (18) or (19)
$\mathbf{D}$	$n_s \times m$ coefficient matrix in rational approximation (eq. (3))
$\mathbf{E}$	$m \times (n_s + n_c + n_g)$ coefficient matrix in rational approximation (eq. (3))
$\mathbf{F}$	$n_s \times (n_s + n_c + n_g)$ real part of tabulated aerodynamic matrices
$\mathbf{F}_s$	$n_s \times 1$ vector of generalized aerodynamic forces (eq. (1))
$\widetilde{\mathbf{F}}$	$n_s \times (n_s + n_c + n_g)$ real part of approximated aerodynamic matrices (eq. (7))
$\overline{\mathbf{F}}$	defined in equations (13b) or (14b)
$\mathbf{G}$	$n_s \times (n_s + n_c + n_g)$ imaginary part of tabulated aerodynamic matrices
$\widetilde{\mathbf{G}}$	$n_s \times (n_s + n_c + n_g)$ imaginary part of approximated aerodynamic matrices (eq. (8))
$\overline{\mathbf{G}}$	defined in equations (18) or (19)
$\mathbf{I}$	unit matrix
$\mathbf{K}_s$	$n_s \times n_s$ generalized structural stiffness matrix
k	reduced frequency, $\omega b/V$
k_f	tabulated reduced frequency at which real-part match constraint is applied
k_g	tabulated reduced frequency at which imaginary-part match constraint is applied
k_ℓ	tabulated reduced frequency
L_g	gust characteristic length
$\mathbf{M}_s$	$n_s \times n_s$ generalized structural mass matrix

$\overline{\mathbf{M}}_s$	$n_s \times n_s$ generalized structural and aerodynamic mass matrix (eq. (6))
m	number of aerodynamic augmented states
n	initial [**D**] method in numerical application
n_c	number of control surface modes
n_g	number of gust modes
n_m	number of measurement points
n_s	number of structural vibration modes
n_{wd}	number of weight-peak widening cycles
$\mathbf{Q}$	$n_s \times (n_s + n_c + n_g)$ matrix of generalized unsteady aerodynamic force coefficients
$\tilde{\mathbf{Q}}$	$n_s \times (n_s + n_c + n_g)$ rational approximation of $\mathbf{Q}$ (eq. (3))
$\overline{\mathbf{Q}}_{ij}$	absolute value of (i,j)th weighted aerodynamic term
$\mathbf{Q}^*_{ij}$	maximum of $\overline{\mathbf{Q}}_{ij}$ values at various tabulated reduced frequencies
p	nondimensionalized Laplace variable, sb/V
q	dynamic pressure
$\mathbf{R}$	$m \times m$ diagonal matrix of aerodynamic roots in rational approximation (eq. (3))
s	Laplace variable
$\mathbf{T}$	$n_c \times n_m$ control-system transfer function matrix, including sensors and actuators
$\mathbf{u}$	$3n_c \times 1$ control vector (eq. (5))
V	true flow velocity
$\mathbf{W}$	matrix of weights assigned to tabulated data
$\widetilde{\mathbf{W}}$	maximum product of the magnitude of an aerodynamic tabular value times its measure of importance (eq. (34))
$\overline{\mathbf{W}}$	measure-of-importance matrix (eqs. (28), (30), and (33))
$\mathbf{w}$	$2n_g \times 1$ gust vector (eq. (5))
w_{cut}	lowest limit of $\mathbf{Q}^*_{ij}$
$\mathbf{w}_g$	$n_g \times 1$ vector of gust velocities
$\mathbf{x}$	$(2n_s + m) \times 1$ state vector (eq. (5))
δ_c	$n_c \times 1$ vector of control-surface deflections (actuator outputs), rad
$\epsilon_{ij\ell}$	weighted approximation error of (i,j)th term in ℓth tabulated matrix (eq. (24))
ϵ_t	total weighted approximation error (eq. (24))
ϵ_{t_N}	total weighted approximation error calculated with weights of equation (25)

ν	arbitrary positive integer
ξ	$n_s \times 1$ vector of generalized displacements of vibration modes
σ_g	gust root-mean-square (rms) velocity
Φ_g	Dryden's power spectral density function
$\boldsymbol{\Psi}_m$	$n_m \times n_s$ sensor-input deflection matrix
$\boldsymbol{\Psi}_z$	$n_g \times n_s$ structural modal deflections at acceleration points for gust weighting
ω	frequency of oscillation

Subscripts:

a	aerodynamic
c	control-surface mode
g	gust velocity mode
ℓ	related to ℓth tabulated reduced frequency (k_ℓ)
s	structural vibration mode

Notation:

$[\,\cdot\,]^T$	transpose of a matrix $[\,\cdot\,]$
$\{\,\cdot\,\}$	column vector
$(\,)_{ij}$	(i,j)th element of matrix indicating ith row, jth column

Acronyms:

AFW	Active Flexible Wing
ELS	extended least squares
EMMP	extended modified matrix-Padé
EMS	extended minimum state
GAF	generalized aerodynamic force
ISAC	Interaction of Structures, Aerodynamics, and Controls system of programs
LS	least squares
MIST	Minimum-State computer program
MMP	modified matrix-Padé
MP	matrix-Padé
MS	minimum state

A dot over a symbol indicates the derivative with respect to time.

Table 1. Minimum-State Aerodynamic Approximation Roots

m	Approximation roots, $\mathbf{R}_i$
2	−0.4, −1.5
4	−0.3, −0.6, −1.1, −1.6
6	−0.2, −0.4, −0.7, −1.0, −1.4, −1.8
8	−0.1, −0.3, −0.5, −0.7, −1.0, −1.3, −1.6, −2.0
10	−0.05, −0.2, −0.4, −0.6, −0.8, −1.0, −1.3, −1.6, −2.0, −2.5
12	−0.05, −0.15, −0.3, −0.45, −0.6, −0.8, −1.0, −1.2, −1.4, −1.7, −2.1, −2.6
15	−0.04, −0.1, −0.2, −0.3, −0.45, −0.6, −0.75, −0.9, −1.1, −1.3, −1.5, −1.7, −2.0, −2.4, −3.0
20	−0.03, −0.09, −0.15, −0.2, −0.3, −0.4, −0.5, −0.6, −0.7, −0.82, −0.95, −1.1, −1.25, −1.4, −1.55, −1.7, −1.9, −2.2, −2.6, −3.1

Table 2. Minimum-State Approximation Errors

Weight method	Initial [**D**] method	w_{cut}	Error parameter	Approximation errors at— $m = 2$	$m = 4$	$m = 6$	$m = 8$	$m = 10$
Data normalization	2		$\epsilon_t = \epsilon_{t_N}$	4.978	2.914	1.938	1.696	1.284
Physical	1	0	ϵ_t	0.523	0.507	0.501	0.488	0.462
			ϵ_{t_N}	10.869	9.820	5.776	7.906	10.653
	2	0	ϵ_t	0.529	0.509	0.502	0.491	0.465
			ϵ_{t_N}	10.211	9.513	6.007	7.713	9.932
	1	0.1	ϵ_t	0.641	0.564	0.549	0.537	0.502
			ϵ_{t_N}	7.544	4.135	3.402	2.715	3.510

Table 3. Approximation Results With Various Constraint Sets

Case	NKF	IRED	ϵ_t	ϵ_{t_N}	q_f, psi	q_f error, percent	ω_f, rad/sec	ω_f error, percent
1	14	0	0.532	4.240	1.347	−0.362	90.904	0.184
2	7	0	.525	15.287	1.353	.096	90.749	.013
3	0	0	.523	11.587	1.355	.281	90.800	.069
4	−2	0	.528	9.984	1.356	.296	90.886	.164
5	−2	4	.569	15.879	1.376	1.805	90.983	.271

Table 4. **IMIST.DAT** Input Parameters

Record	Description		
1	NC, NR, NSKIP, N1, N2, M, NK, NKF, ITMAX, NPR, IFILE, IWE, ISTAB, IRED		
	NC		Number of columns in the tabulated aerodynamic matrices on TABAERO.DAT $(0 < NC \leq 40)$
	NR		Number of rows in the tabulated aerodynamic matrices on TABAERO.DAT $(0 < NR \leq 40)$
	NSKIP	≥ 0	Number of first modes whose data on TABAERO.DAT is to be skipped
		< 0	NG = −NSKIP. The last NG (out of N1) columns are gust related. $(-3 \leq NSKIP < N2)$
	N1		Number of columns to be approximated $(0 < N1 \leq NC)$
	N2		Number of rows to be approximated $(0 < N2 \leq NR)$
		Note:	The number of control modes is (N1 − N2) or (N1 − N2 + NSKIP) when NSKIP < 0.
	M		Number of approximation roots $(0 \leq M \leq 30)$
	NK		Number of tabulated reduced frequencies (k) $(2 < NK \leq 15)$
	NKF	$= 1$	All real and imaginary parts are matched at k(NK).
		> 1	All real and imaginary parts are matched at k(NKF).
		$= 0$	Real parts are matched at k(NK) and imaginary parts at $k(2)$.
		< 0	$[\mathbf{A}_2] = 0$; imaginary parts are matched at $k(-NKF)$.
			Note: See appendix A for discussion on constraints.
	ITMAX		Number of **D**→**E**→**D** iterations (ITMAX > 0)
	NPR	> 0	Write approximated aerodynamic terms on file RES.DAT at all tabulated k values (except $k = 0$) and at (NPR − 1) intermediate k values for each interval.
		< 0	Write absolute values of weighted tabulated aerodynamics on file RES.DAT.
	IFILE	$\neq 0$	Write approximation matrices on SPLANE.DAT and on SPLCOF.DAT.
		< 0	Write weight matrices on IM.DAT.

Table 4. Concluded

Record	Description		
1 (contd)	IWE	= 1	Use weight matrices from a previous run.
		= 2	Calculate weight matrices based on physical weighting.
		= 3	Calculate weight matrices for data normalization.
	ISTAB	> 0	Create file T5STAB_INT.DAT with no sensors.
		= 0	Do not create T5STAB_INT.DAT.
		< 0	Create file T5STAB_WT.DAT with −ISTAB sensors.
		Note:	If IRED ≠ 0, the program sets ISTAB = 0.
	IRED		Number of highest frequency modes that are candidates for dynamic reduction (0 ≤ IRED < N2)
If M = 0, the rest of the file is not required.			
2	R(I), I = 1, M		Approximation roots (diagonal of [**R**]). Distinct negative values
Record 3 is repeated for I = 1, N2.			
3	D(I, J), J = 1, M		The Ith row $\mathbf{D}_i$ of the initial guess for [**D**] where $\mathbf{D}_i \neq 0$ and rank [**D**] = min (**M**, N2)
If IWE ≠ 1, the rest of the file is not required.			
4	PNOR(I), I = 1, N1		Internal mode normalization vector created in a previous run
Records 5 and 6 are repeated for K = 1, NK − 1.			
5	QA(K)		The (**K** + 1)th tabulated k
Record 6 is repeated for J = 1, N1.			
6	WE(I, J, K), I = 1, N2		The Jth column of the weight matrix related to the (**K** + 1)th tabulated k

Table 5. **TABF.DAT** Input Parameters

Record	Description	
1	B, RO, V, PI, WCUT, NWD	
	B	Reference semichord (b) used in generating the tabulated aerodynamic matrices
	RO	Air density at the design point for physical weighting (ρ)
	V	True airspeed at the design point (V)
	PI	π
	WCUT	The minimal maximum absolute value of each weighted aerodynamic term, $\overline{\mathbf{Q}}_{ij}$ (w_{cut} of eq. (31)) $(0 \leq \text{WCUT} \leq 1)$
	NWD	Number of weight-peak widening cycles. In each cycle, all the physical $\mathbf{W}_{ij\ell}$ values are set to be equal to $\max\{\mathbf{W}_{ij(\ell-1)}, \mathbf{W}_{ij\ell}, \mathbf{W}_{ij(\ell+1)}\}$ of the previous cycle. $(0 \leq \text{NWD} \leq \text{NK} - 2)$
2	FR(I), I = 1, NR	Natural frequencies (in Hz) of the vibration modes, supplemented by zeros for the control modes
3	Dummy record	
4	(GM(I, J), I = 1, NR), J = 1, NR	The generalized mass matrix $\begin{bmatrix} \mathbf{M}_{ss} & \mathbf{M}_{sc} \\ \mathbf{M}_{sc}^T & \mathbf{M}_{cc} \end{bmatrix}$
5	Dummy record	
6	DA(I), I = 1, NR	Dimensionless modal damping of the vibration modes, supplemented by zeros for the control modes
	If NSKIP $\geq$ 0 (no gust columns), the rest of the file is not required.	
7	ELG	Gust length scale (L_g)
	Records 8 and 9 are repeated for J = 1, NG where NG = −NSKIP.	
8	SWG(J)	Jth continuous gust root-mean-square value (σ_g^2) (SWG(J) > 0)
	Note:	Only the ratio between different SWG(J) values affects the results.
9	XI(J, I), I = 1, N2	Modal deflections at a structural point selected for weighting the Jth gust column $\left(\lfloor \mathbf{\Psi}_{z_j} \rfloor\right)$ $\left(\lfloor [\mathbf{\Psi}_{z_j}] \neq [0] \rfloor\right)$

Table 6. **TABAERO.DAT** Input Parameters

Record	Description
1	QAY(J, I), I = 1, NK Tabulated reduced frequencies (k_ℓ) ($k_1 = 0$)
Record 2 is repeated for **I** = 1, NK.	
2	(AR(J, K, I), AI(J, K, I), J = 1, NR), K = 1, NC Real and imaginary parts of the tabulated aerodynamic matrices, given column by column

Table 7. **TRAN.DAT** Input Parameters

Record	Description
1	NS Number of sensors ($0 < NS \leq 4$)
Records 2 and 3 are repeated for I = 1, NS.	
2	NP(I) = 0 Deflection sensor = 1 Rate sensor = 2 Acceleration sensor
3	FI(I, J), J = 1, N2 Modal deflections or rotations at the location of the Ith sensor ($\lfloor \Psi_{m_i} \rfloor$) ($\lfloor \Psi_{m_i} \rfloor \neq \lfloor 0 \rfloor$)
Records 4 and 5 are repeated for I = 1, N3, where N3 = N1 − N2 − NG.	
4	GAIN(I) Gain of the Ith control mode (>0)
5	ACT(I, J), J = 1, 3 Coefficients of the Ith actuators whose transfer function is defined by $\mathbf{T}_{act} = \frac{GAIN(I) * ACT(I, 1)}{S^3 + ACT(I, 3) * S^2 + ACT(I, 2) * S + ACT(I, 1)}$

Table 8. **T5STAB_TAB.DAT** Input Parameters

Record	Description	
1	QAY(I), I = 1, N	Tabulated reduced frequencies (k_ℓ). Values of k_ℓ at which match constraints are not imposed may be different from those in TABAERO.DAT.
Record 2 is repeated NR × NC × NK times.		
2	AP1(I, J, K), AP2(I, J, K)	Real and imaginary parts of the (I, J)th term of the Kth tabulated aerodynamic matrix. These values are ignored by the program.
3	(GM(I, J), I = 1, NR), J = 1, NR	Generalized mass matrix
4	FR(I), I = 1, NR	Natural frequencies (in Hz)
5	D(I), I = 1, NR	Modal structural dampings
If ISTAB ≥ 0, the rest of the file is not required. Record 6 is repeated for J = 1, NS where NS = − ISTAB.		
6	FI(I, J), I = 1, NR	Modal deflections at the location of the Jth sensor ($\lfloor \Psi_{m_j} \rfloor$)

Table 9. User-Console Output Parameters

Record	Description	
If IWE $\neq$ 2, records 1–4 are not typed.		
1	B, RO, V, PI, WCUT, NWD, Q	
	B, RO, V, PI, WCUT, NWD	The parameters of TABF.DAT, record 1 (table 5)
	Q	The dynamic pressure, based on RO and V
Record 2 is repeated for I = 1, N2.		
2	FR(I), GM(I), DA(I), PNOR(I)	
	FR(I)	The Ith natural frequency from TABF.DAT
	GM(I)	The Ith generalized mass from TABF.DAT
	DA(I)	The Ith modal damping from TABF.DAT
	PNOR(I)	A division factor that normalizes the modes to unit generalized mass. PNOR(I) = SQRT(GM(I)). This is an internal process. The results are renormalized before being output.
Record 3 is repeated for I = 2, NK.		
3	DETE, FRK(I)	
	DETE	A complex output parameter of subroutine DCXINV. A value other than (1, 0) or (−1, 0) indicates numerical problems in the complex matrix inversion.
	FRK(I)	The frequency associated with the Ith tabulated k, $k(V/2\pi b)$
4	P, P1, P2	The percentage of small weighted aerodynamic terms that are affected by w_{cut} in equation (31), for each weighting group separately (vibration mode, controls, and gusts)
Record 5 is repeated ITMAX times (once for each [**D**]→[**E**]→[**D**] iteration).		
5	ITER, ER, ERI	
	ITER	Iteration number
	ER	Total approximation error (eq. (24))
	ER1	Total approximation error calculated with data normalization weighting of equation (25)
	Note:	When IWE = 3, ER = ER1. Increasing ER indicates numerical problems in the [**D**]→[**E**]→[**D**] iterations.
Record 6 is typed only if IFILE $\neq$ 0.		
6	NLAST	The number of words written on SPLCOF.DAT: NLAST = (M + 3) * NR * N1 + M * (N1 + N2)

Table 10. **SPLANE.DAT** Output Parameters

Record	Description
Record 1 is repeated for $\mathbf{L} = 1, \mathbf{M} + 3$.	
1	(F(I, J, L), J = 1, N1), I = 1, N2 The $[\mathbf{A}_{\gamma+2}]$ coefficient matrix, with $\gamma = \mathbf{L} - 3$, of the approximation in equation (3), expanded in the form: $[\tilde{\mathbf{Q}}(p)] = [\mathbf{A}_0] + [\mathbf{A}_1]p + [\mathbf{A}_2]p^2 + \sum_{\gamma=1}^{M} \frac{[\mathbf{A}_{\gamma+2}]}{p-\mathbf{R}_\gamma}$ where, starting with $\gamma = 1, [\mathbf{A}_{\gamma+2}] = \{\mathbf{D}_\gamma\}[\mathbf{E}_\gamma]$. This expansion is required for approximation curve plotting by SPLFIT.
2	(D(I, L), L = 1, M), I = 1, N2 The final [**D**]
3	(E(L, J), J = 1, N1), L = 1, M The final [**E**]
4	N2, N1, M N2 Number of rows of approximated aerodynamic matrix N1 Number of columns of approximated aerodynamic matrix M Number of aerodynamic roots
5	−R(L), L = 1, M Aerodynamic approximation roots, with inverted sign to be consistent with ISAC's formulation

Table 11. **RES.DAT** Output Parameters

Record	Description
1	NC, NR, NSKIP, N1, N2, M, NK, NKF, ITMAX, NPR, IFILE, IWE, ISTAB, IRED Run parameters, first record of IMIST.DAT
2	−R(L), L = 1, M — Aerodynamic approximation roots, with inverted sign
3	QAY(I), I = 1, NK — Tabulated reduced frequencies
Record 4 is repeated ITMAX times.	
4	ITER, ER, ER1 — Approximation errors, same as record 5 of table 9
Record 5 is repeated for I = 1, N2.	
5	D(I, J), J = 1, M — The Ith row of the final [**D**]
Record 7 is repeated for I = 1, M.	
7	E(I, J), J = 1, N1 — The Ith row of the final [**E**]
Records 8 and 9 are written only if NPR < 0. Repeat for **K** = 2, NK.	
8	QAY(K) — The **K**th tabulated k
9	(WEQ(I, J), I = 1, N2), J = 1, N1 Absolute values of the **K**th-weighted tabulated aerodynamic matrix
Records 10 and 11 are written only if NPR > 0. They are repeated N2 × N1 times.	
10	I, J — Row and column identification numbers
Record 11 is repeated (NK − 1) * NPR + 1 times.	
11	Q, ARR, AP1, AAI, AP2, ER1 Q — The interpolated k value ARR — Real part of the (i, j) tabulated aerodynamic term AP1 — Real part of the (i, j) approximated aerodynamic term AAI — Imaginary part of the (i, j) tabulated aerodynamic term AP2 — Imaginary part of the (i, j) approximated aerodynamic term ER1 — Squared approximation error of the (i, j) term Note: — ARR, AAI, and ER1 are calculated at tabulated k values only.

Table 12. **SPLCOF.DAT** Output Parameters

Record	Description
Record 1 is repeated for J = 1, N1.	
1	(F(I, J, L), I = 1, NR), L = 1, M + 3 Approximation coefficient matrices. Same as record 1 of SPLANE.DAT (table 10) with two exceptions: (1) the matrices here are given in a different order, and (2) the matrices are supplemented by zero terms for the NR–N2 bottom rows.
2	(D(I, L), I = 1, N2), L = 1, M — The final [**D**], column by column
3	(E(L, J), L = 1, M), J = 1, N1 — The final [**E**], column by column

Table 13. **IMIST.DAT** for the Sample Case

(NC	NR	NSKIP	N1	N2	M	NK	NKF	ITMAX	NPR	IFILE	IWE	ISTAB	IRED)
16	15	−1	16	11	4	14	1	30	0	1	2	0	0
	−0.300			−0.600		−1.100		−1.600					($\mathbf{R}_i$)
	1085.242			−2771.134			766.4360			−273.9914			
	−0.9773058			2.497540			−0.5862706			0.2077749			
	4.230847			−5.392477			0.4645342			−0.2338193			
	2.012684			−4.920019			1.834980			−0.7853356			
	−0.9957080			3.737066			−1.985531			1.092124			(initial [**D**])
	−13.57052			17.89878			−1.509577			−0.5197472			
	−6.311030			3.913992			0.9018466			−0.9920467			
	11.30995			−7.358065			−2.402427			2.099382			
	5.715536			−5.240108			−0.5718663			0.9348391			
	4.989137			−6.978589			0.3833005			0.9326578			
	2.287535			−2.101954			−0.3638385			0.6776571			

Table 14. **TRAN.DAT** for the Sample Case

1					(NS)
1					(NP(1))
1.0000	−7.92027E-05	−2.80898E-03	−4.16988E-04	2.04932E-03	
1.18939E-03	−9.40258E-04	8.20041E-04	3.60080E-05	5.17672E-05	$(\lfloor \mathbf{\Psi}_{m_i} \rfloor)$
1.23072E-03					
0.001					
6751689.	66157.39	259.97			
−0.1					
6800581.	70406.67	325.39			(Gains and actuator coefficients)
0.1					
10867040.	90678.24	358.43			
−0.1					
17462768.	136576.6	217.40			

Table 15. **TABF.DAT** for the Sample Case

(B	RO	V	PI	WCUT	NWD)
19.88	09888E−6	5508.	3.14159	0.1	0

.000000
7.105512
8.727085
15.893922
16.939290
27.929165
38.391348
39.638754 (Natural frequencies)
44.763802
49.371975
49.917961
0.
0.
0.
0.

GMASS

128.429	0.0000000E+00	0.0000000E+00	0.0000000E+00	0.0000000E+00
0.0000000E+00	0.0000000E+00	0.0000000E+00	0.0000000E+00	0.0000000E+00
0.0000000E+00	−0.2768736E+00	−0.2614632E+00	−0.1412688E+00	−0.1368480E+00
0.0000000E+00	0.2590083E−02	0.0000000E+00	0.0000000E+00	0.0000000E+00
0.0000000E+00	0.0000000E+00	0.0000000E+00	0.0000000E+00	0.0000000E+00
0.0000000E+00	−0.3539690E−03	−0.1034990E−02	−0.5807050E−03	−0.9522450E−03
0.0000000E+00	0.0000000E+00	0.2590083E−02	0.0000000E+00	0.0000000E+00
0.0000000E+00	0.0000000E+00	0.0000000E+00	0.0000000E+00	0.0000000E+00
0.0000000E+00	−0.5042240E−04	−0.2872990E−03	−0.1701440E−03	−0.3128950E−03
		:		
		:		
0.8494820E−03	−0.9037930E−03	0.1543230E−02	−0.5283170E−02	0.1339410E−02
−0.9004400E−03	0.3764320E−01	0.0000000E+00	0.0000000E+00	0.0000000E+00
−0.2614632E+00	−0.1034990E−02	−0.2872990E−03	0.6395270E−03	−0.1581130E−03
0.8873140E−03	0.4341100E−02	−0.5119100E−03	0.2136360E−02	−0.2563590E−02
−0.6568000E−02	0.0000000E+00	0.4349060E−01	0.0000000E+00	0.0000000E+00
−0.1412688E+00	−0.5807050E−03	−0.1701440E−03	0.6145630E−03	−0.2776430E−03
−0.2714550E−03	0.2321360E−03	0.2367750E−03	−0.7962690E−03	0.2473540E−03
0.1544600E−03	0.0000000E+00	0.0000000E+00	0.7372500E−02	0.0000000E+00
−0.1368480E+00	−0.9522450E−03	−0.3128950E−03	−0.1568180E−03	0.6420640E−05
0.1450120E−03	0.1221410E−02	0.5424900E−05	0.4291470E−03	0.6727150E−04
0.1443590E−02	0.0000000E+00	0.0000000E+00	0.0000000E+00	0.8953550E−02

DAMPINGS

0.00	0.03	0.03	0.03	0.03	0.03	0.03	0.03	0.03	0.03	0.03
0.00	0.00	0.00	0.00							

1200. (L_g)

1. (σ_g^2)

−47.9085	6.92438E−02	−2.42383E−01	−1.25759E−01	2.03764E−01
−1.00761E−01	2.03161E−02	−6.98395E−02	−4.04137E−03	2.27311E−02 $\left(\lfloor \Psi_{z_j} \rfloor\right)$
−3.90583E−03	0.0	0.0	0.0	0.0

Table 16. User-Console Printout

(B	RO	V	PI	Q)
19.88000	9.8880001E−08	5508.000	3.141590	1.499914

(WCUT	NWD)
0.1000000	0

(FR	GM	DA	PNOR)
0.0000000E+00	128.4290	0.0000000E+00	11.33265
7.105512	2.5900831E−03	2.9999999E−02	5.0892860E−02
8.727085	2.5900831E−03	2.9999999E−02	5.0892860E−02
15.89392	2.5900831E−03	2.9999999E−02	5.0892860E−02
16.93929	2.5900831E−03	2.9999999E−02	5.0892860E−02
27.92916	2.5900831E−03	2.9999999E−02	5.0892860E−02
38.39135	2.5900831E−03	2.9999999E−02	5.0892860E−02
39.63876	2.5900831E−03	2.9999999E−02	5.0892860E−02
44.76380	2.5900831E−03	2.9999999E−02	5.0892860E−02
49.37197	2.5900831E−03	2.9999999E−02	5.0892860E−02
49.91796	2.5900831E−03	2.9999999E−02	5.0892860E−02

(DETE	$kV/2\pi b$)
(1.00000000000000,0.000000000000000E+000)	0.2204794
(1.00000000000000,0.000000000000000E+000)	0.4409588
(1.00000000000000,0.000000000000000E+000)	2.204794
(1.00000000000000,0.000000000000000E+000)	4.409588
(1.00000000000000,0.000000000000000E+000)	8.819177
(1.00000000000000,0.000000000000000E+000)	13.22876
(1.00000000000000,0.000000000000000E+000)	17.63835
(1.00000000000000,0.000000000000000E+000)	22.04794
(1.00000000000000,0.000000000000000E+000)	26.45753
(1.00000000000000,0.000000000000000E+000)	35.27671
(1.00000000000000,0.000000000000000E+000)	44.09588
(1.00000000000000,0.000000000000000E+000)	66.14382
(1.00000000000000,0.000000000000000E+000)	88.19176

PERCENTAGE OF SMALL WEIGHTS IS 78.51 86.36 63.64
THE ERROR IN ITER. 1 IS 0.5753782E+00 NORM. ERROR IS 3.767044
THE ERROR IN ITER. 2 IS 0.5691916E+00 NORM. ERROR IS 3.985827
THE ERROR IN ITER. 3 IS 0.5661231E+00 NORM. ERROR IS 4.091323
THE ERROR IN ITER. 4 IS 0.5652547E+00 NORM. ERROR IS 4.124926
THE ERROR IN ITER. 5 IS 0.5647669E+00 NORM. ERROR IS 4.135364
THE ERROR IN ITER. 6 IS 0.5644447E+00 NORM. ERROR IS 4.138480
THE ERROR IN ITER. 7 IS 0.5642145E+00 NORM. ERROR IS 4.140104
THE ERROR IN ITER. 8 IS 0.5640404E+00 NORM. ERROR IS 4.142152
THE ERROR IN ITER. 9 IS 0.5639035E+00 NORM. ERROR IS 4.144952
THE ERROR IN ITER. 10 IS 0.5637924E+00 NORM. ERROR IS 4.148385
THE ERROR IN ITER. 11 IS 0.5637015E+00 NORM. ERROR IS 4.152224
THE ERROR IN ITER. 12 IS 0.5636257E+00 NORM. ERROR IS 4.156291
THE ERROR IN ITER. 13 IS 0.5635620E+00 NORM. ERROR IS 4.160402
THE ERROR IN ITER. 14 IS 0.5635078E+00 NORM. ERROR IS 4.164399
:
THE ERROR IN ITER. 26 IS 0.5632138E+00 NORM. ERROR IS 4.198888
THE ERROR IN ITER. 27 IS 0.5632033E+00 NORM. ERROR IS 4.200768
THE ERROR IN ITER. 28 IS 0.5631942E+00 NORM. ERROR IS 4.202514
THE ERROR IN ITER. 29 IS 0.5631857E+00 NORM. ERROR IS 4.204222
THE ERROR IN ITER. 30 IS 0.5631785E+00 NORM. ERROR IS 4.205831
NO. OF WORDS = 1788
FORTRAN STOP

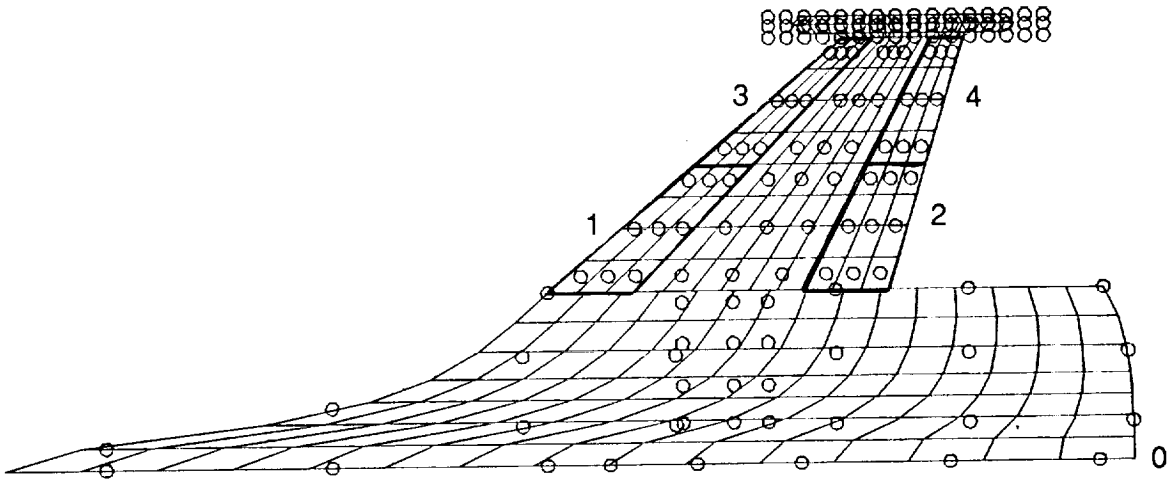

Figure 1. Top view of AFW aerodynamic model.

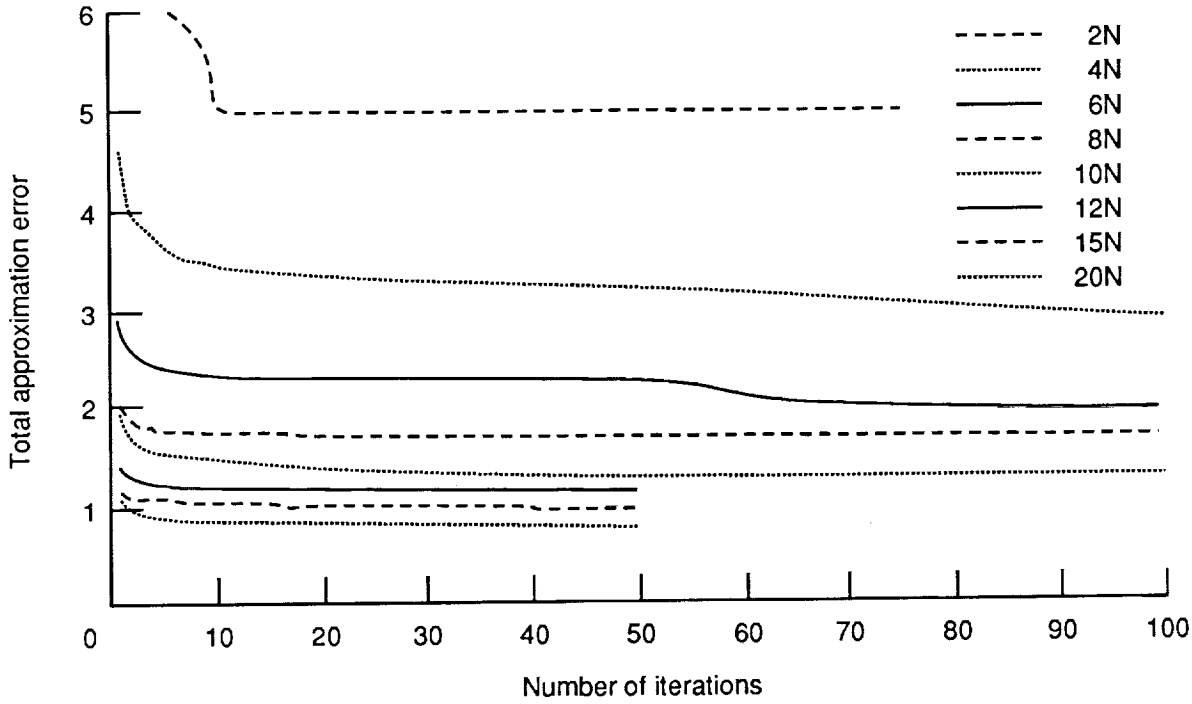

Figure 2. Minimum-state error convergence versus number of iterations for data normalization cases.

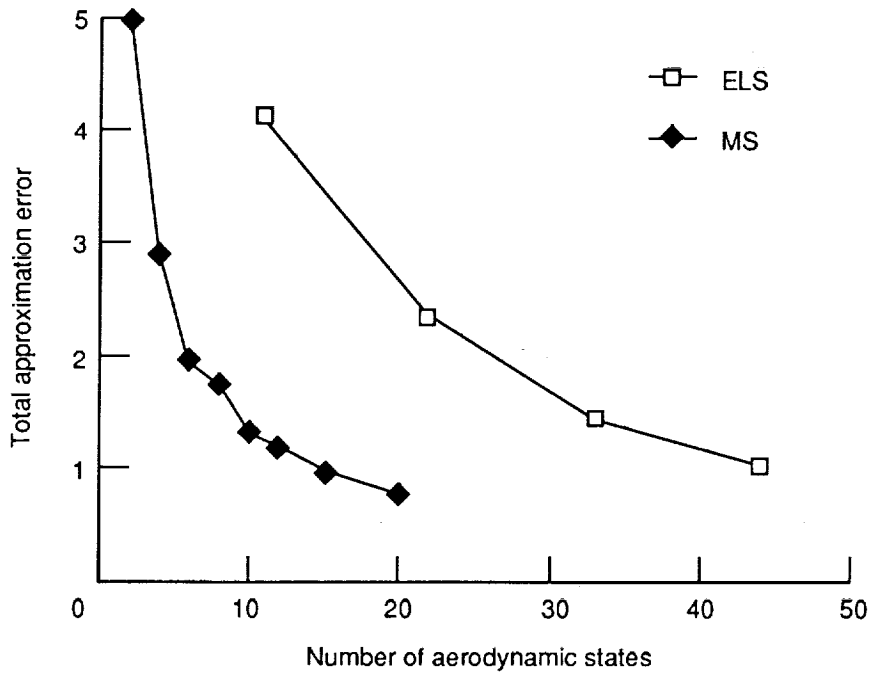

Figure 3. Total approximation errors for minimum-state and extended least-squares methods versus number of aerodynamic lag states.

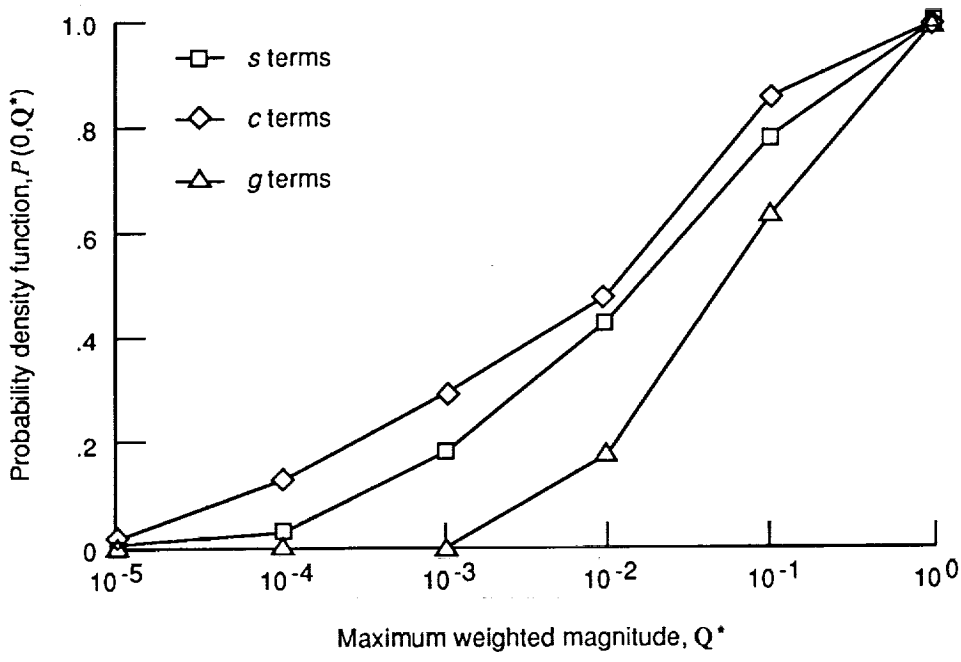

Figure 4. Probability density function of maximum magnitudes of weighted aerodynamic terms.

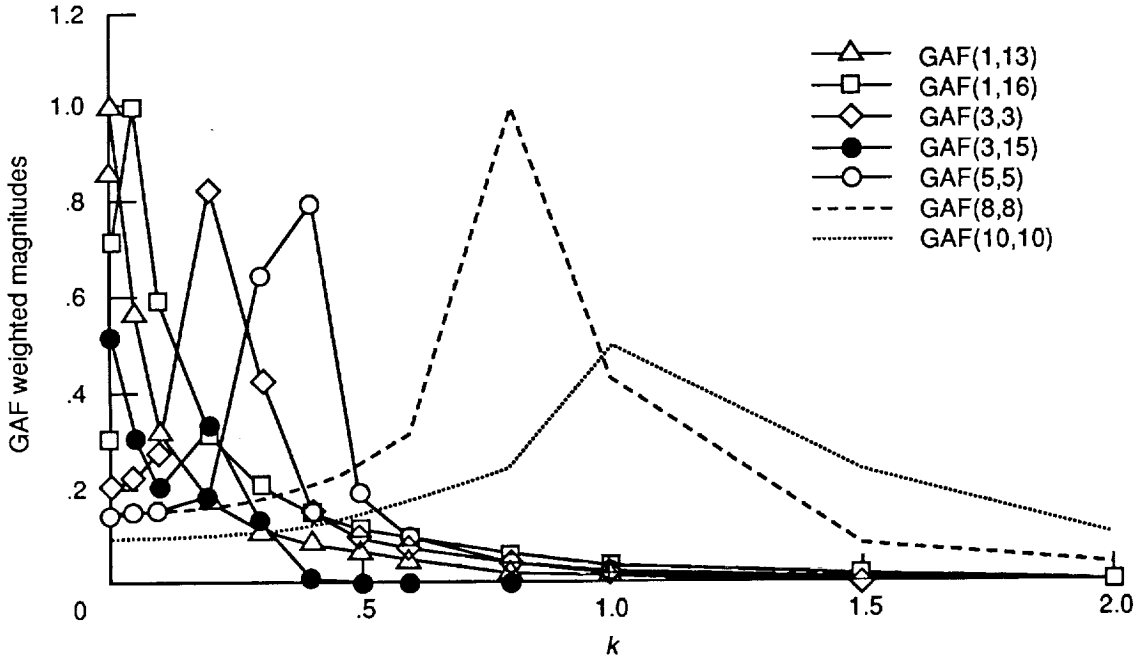

Figure 5. Weighted magnitudes of aerodynamic terms versus reduced frequency.

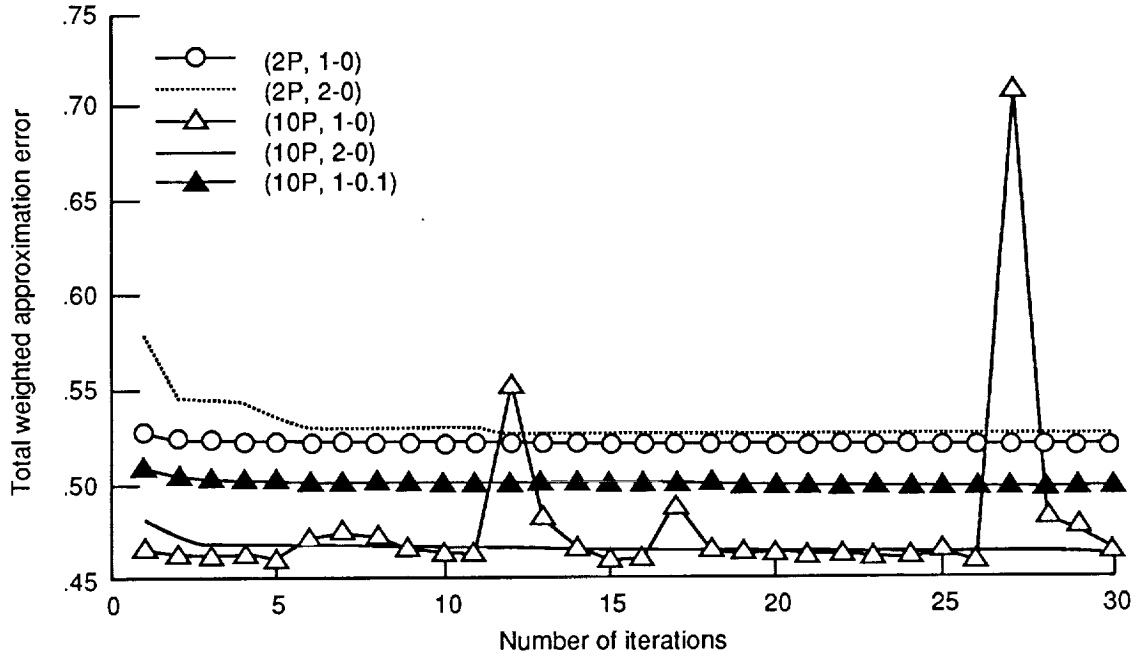

Figure 6. Minimum-state error convergence versus number of iterations in physically weighted cases.

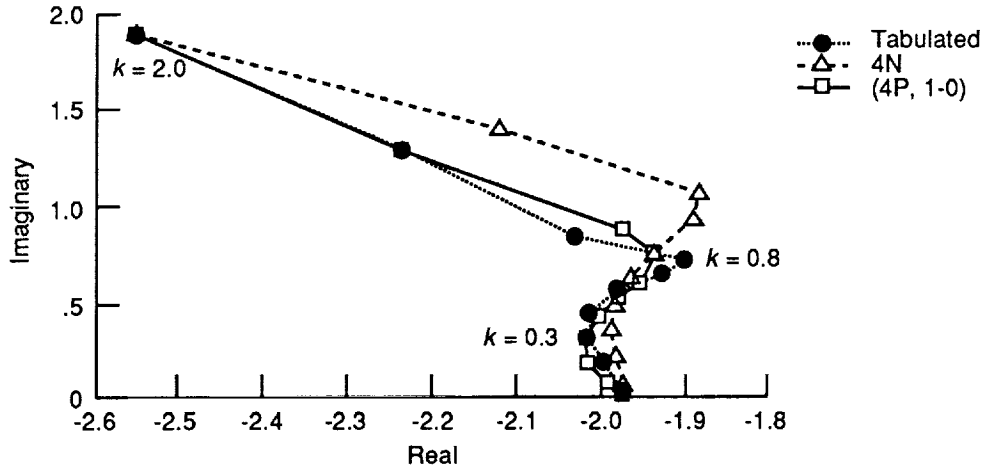

(a) Vibration mode term, GAF(5, 5).

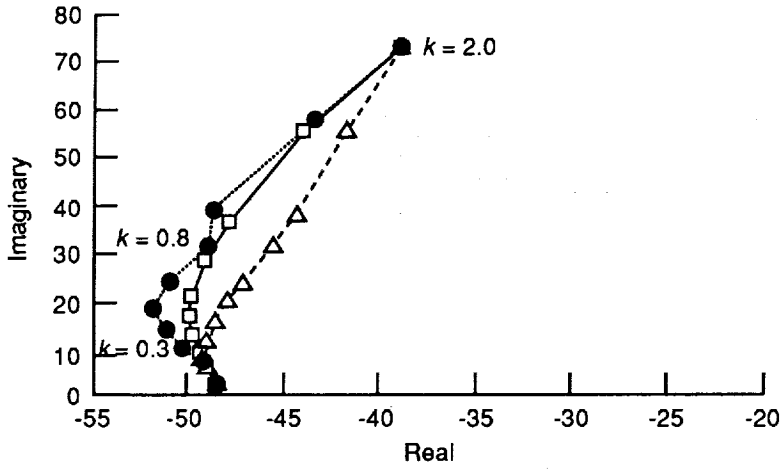

(b) Control mode term, GAF(3, 15).

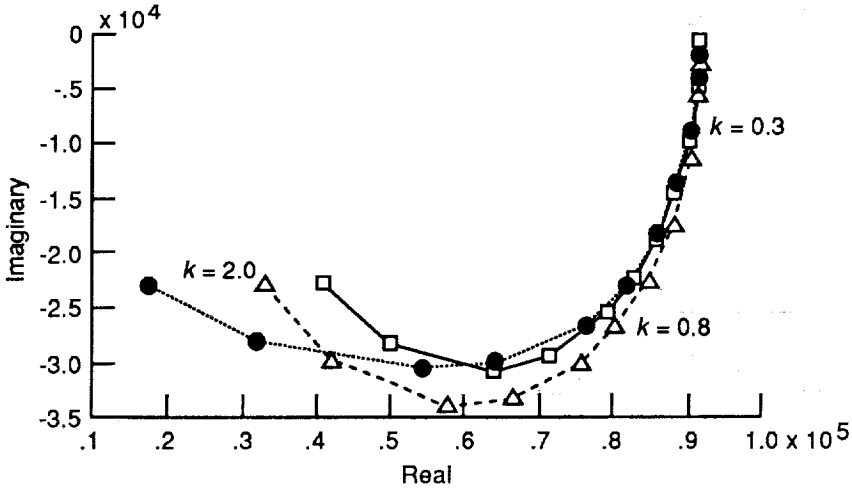

(c) Gust mode term, GAF(1, 16).

Figure 7. Minimum-state curve fits for structural-, control-, and gust-related aerodynamic terms.

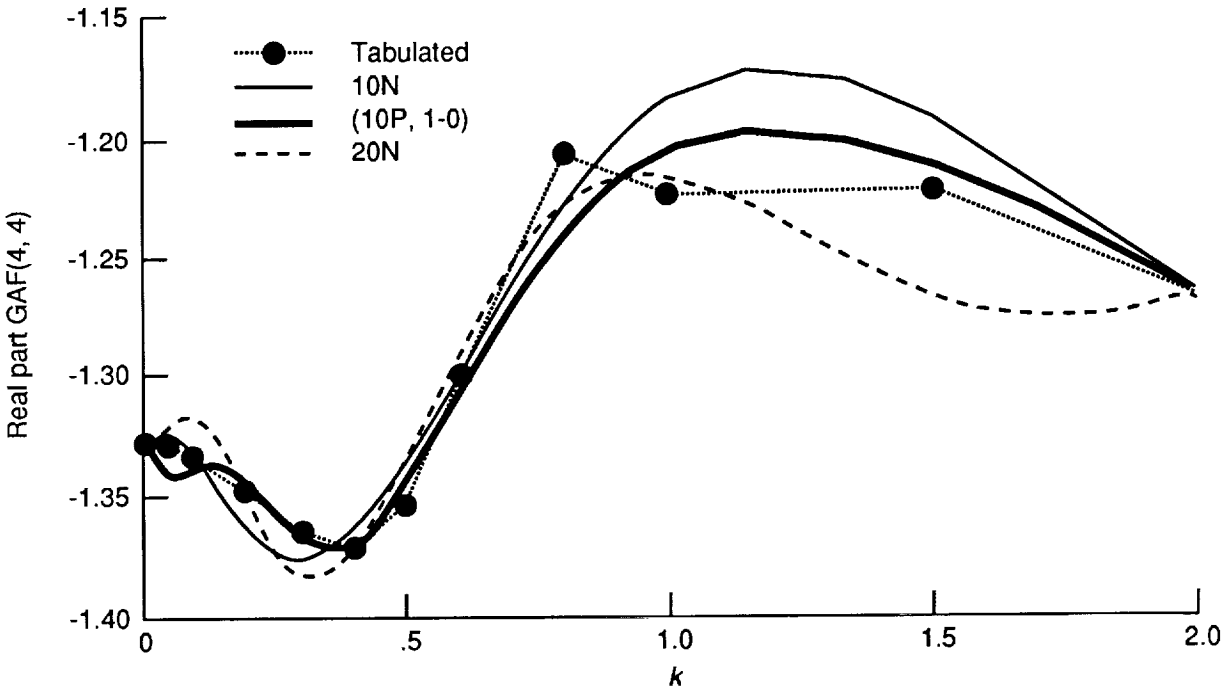

Figure 8. High-order, minimum-state approximation curve fits of real part of $\mathbf{Q}_{4,4}$.

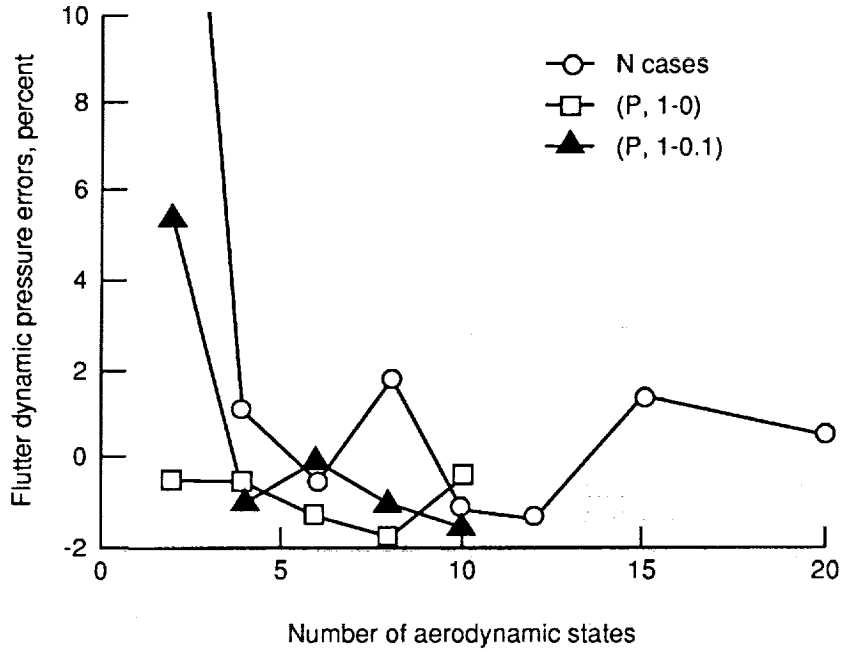

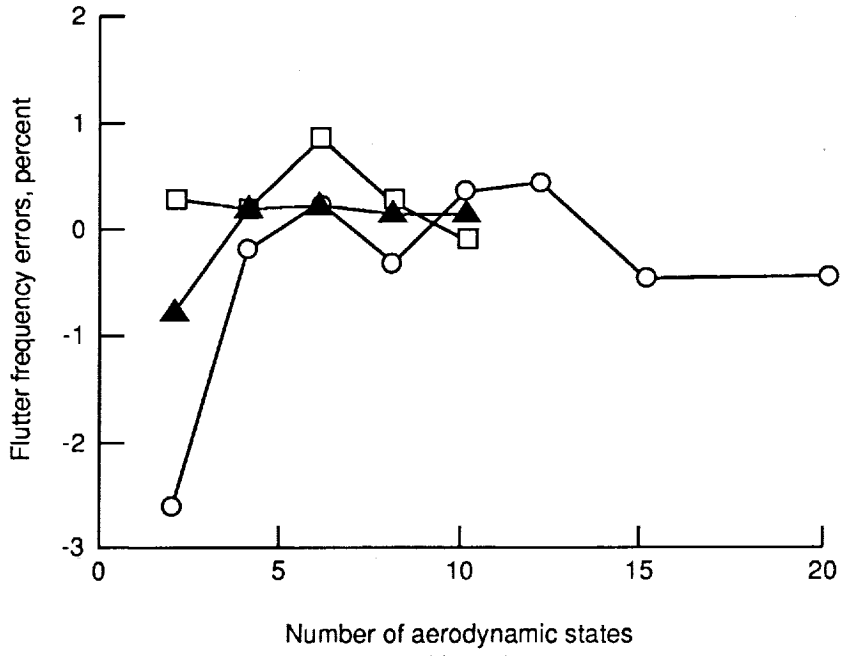

(a) Open loop.

Figure 9. Flutter dynamic pressure and frequency errors using various minimum-state approximations.

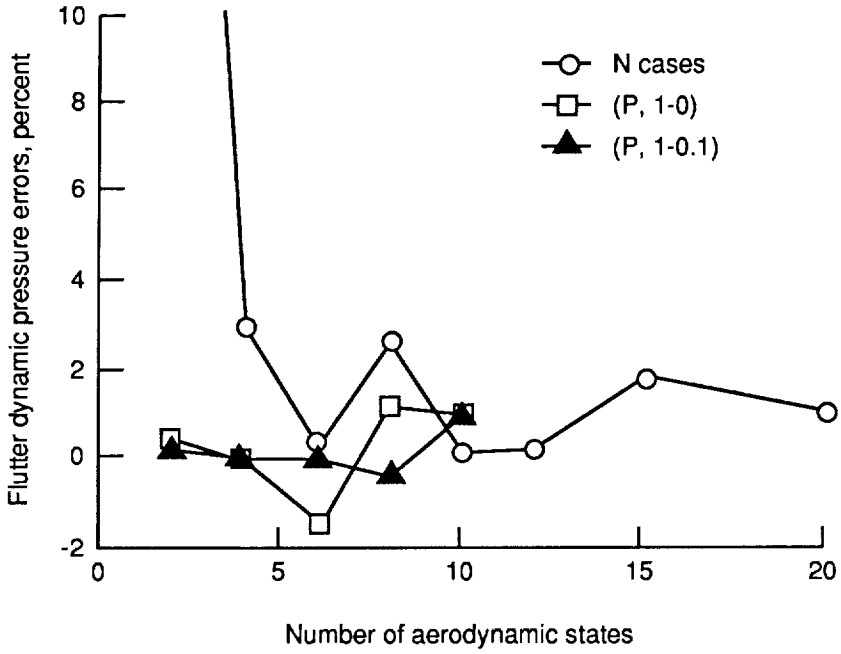

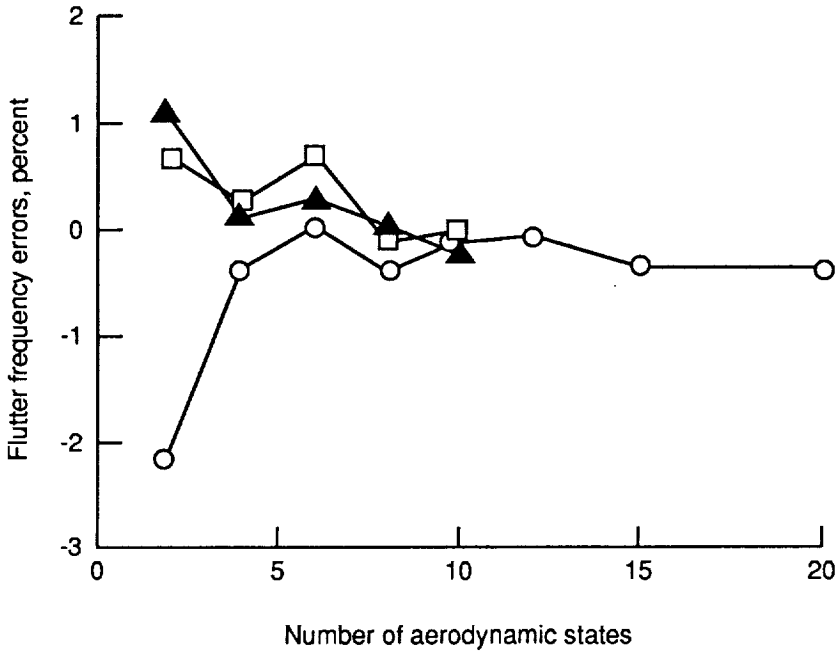

(b) Closed loop.

Figure 9. Concluded.

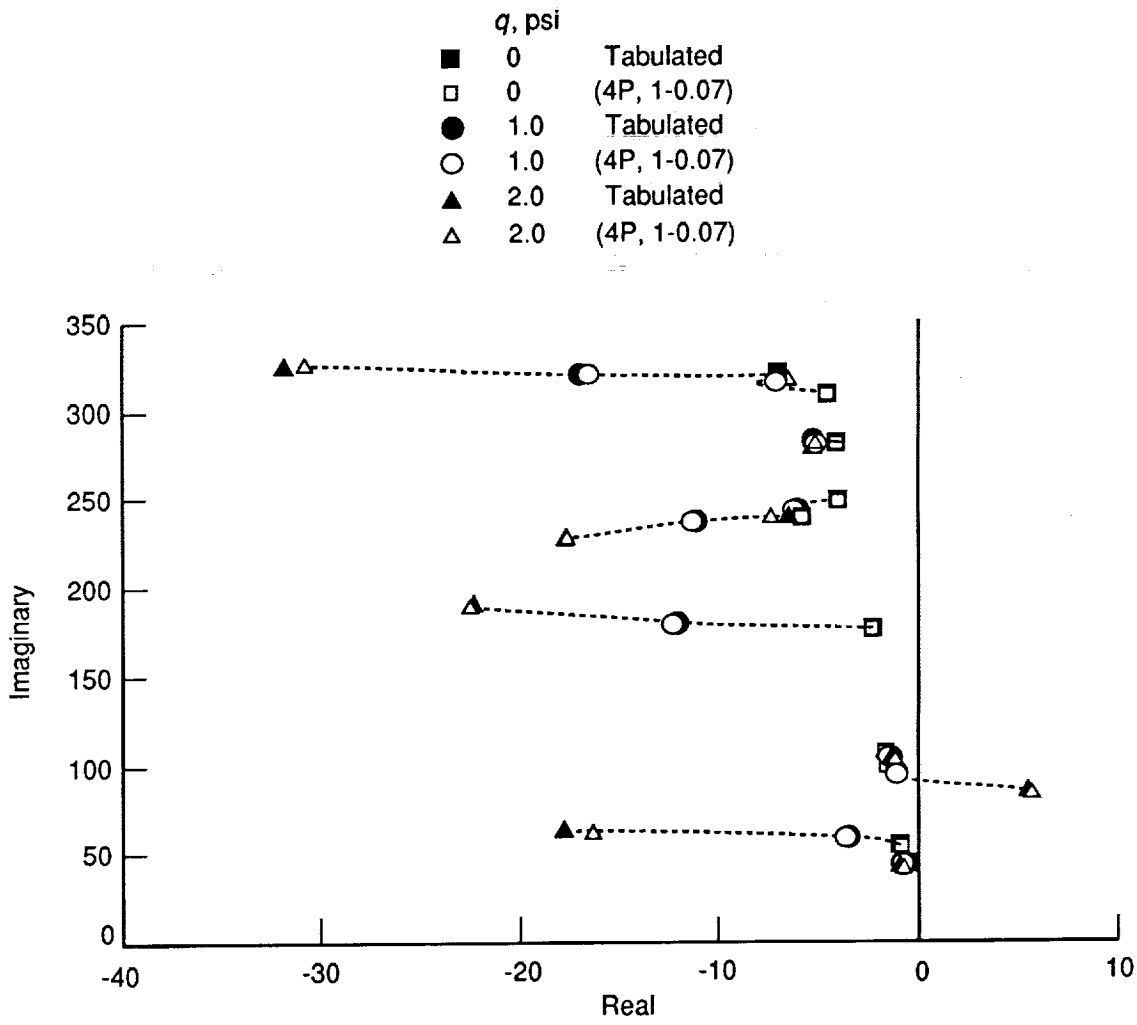

Figure 10. First- and second-order root loci versus dynamic pressure of closed-loop system.

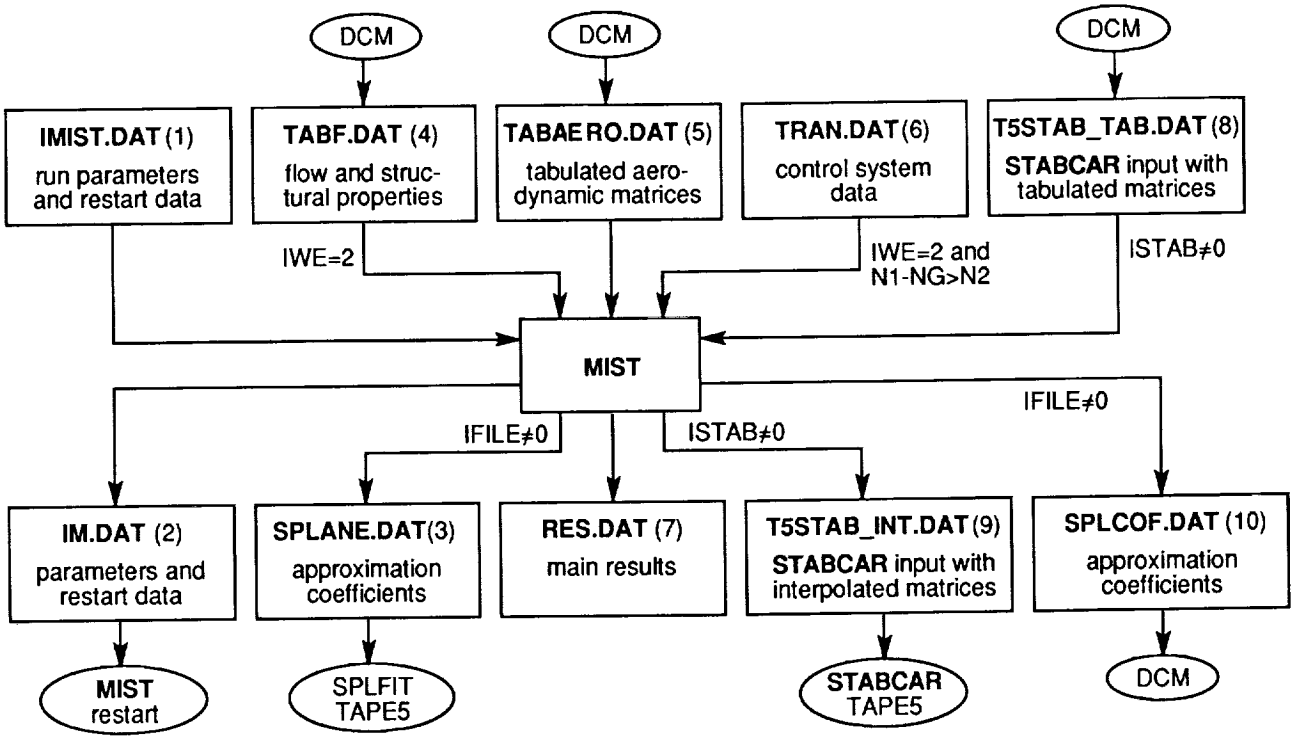

Figure 11. MIST input and output files.

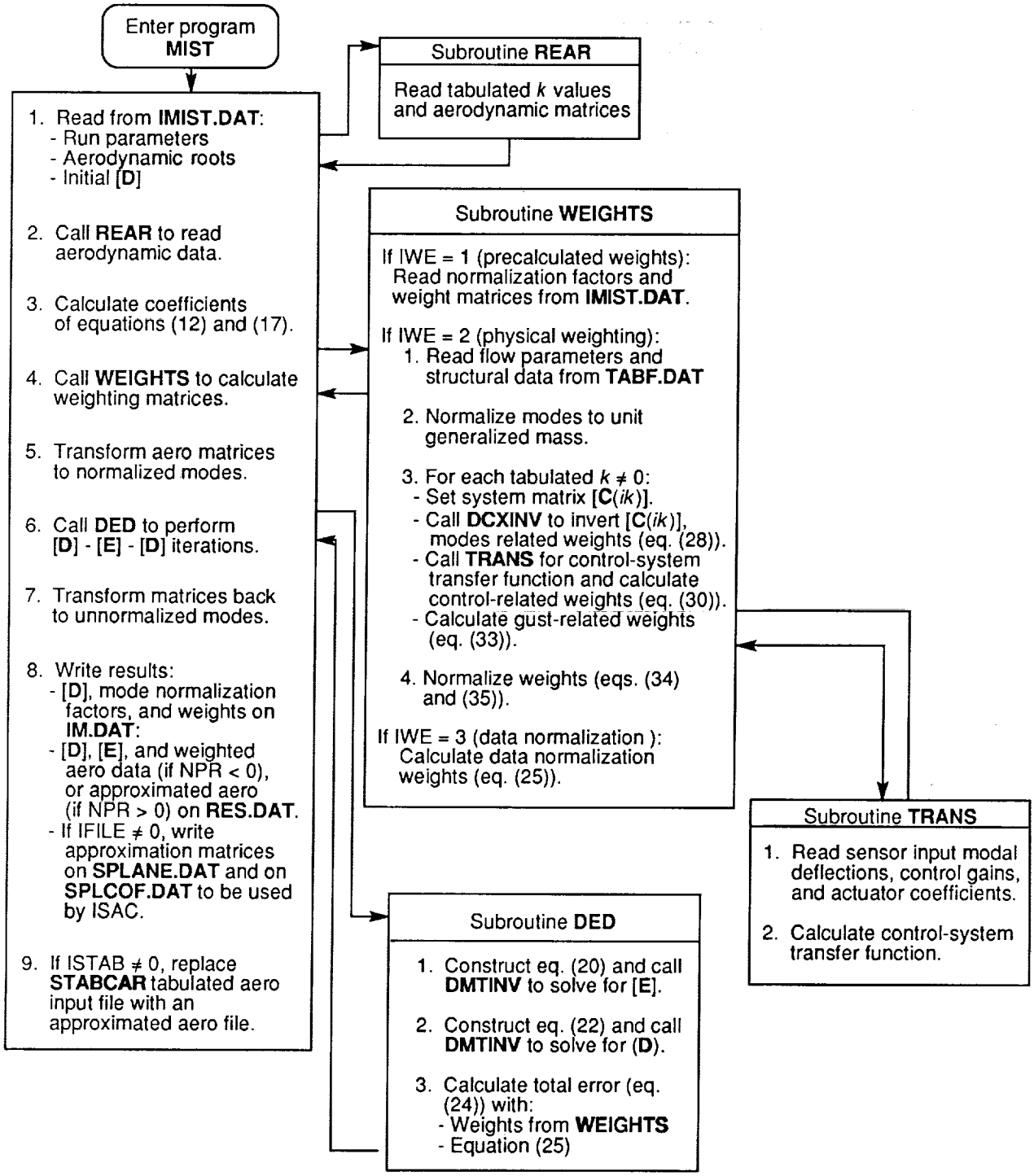

Figure 12. MIST flowchart.

NASA
National Aeronautics and Space Administration

Report Documentation Page

1. Report No.	2. Government Accession No.	3. Recipient's Catalog No.
NASA TP-3025		

4. Title and Subtitle	5. Report Date
Physically Weighted Approximations of Unsteady Aerodynamic Forces Using the Minimum-State Method	March 1991
	6. Performing Organization Code
7. Author(s)	8. Performing Organization Report No.
Mordechay Karpel and Sherwood Tiffany Hoadley	L-16491
9. Performing Organization Name and Address	10. Work Unit No.
NASA Langley Research Center Hampton, VA 23665-5225	505-63-21-04
	11. Contract or Grant No.
12. Sponsoring Agency Name and Address	13. Type of Report and Period Covered
National Aeronautics and Space Administration Washington, DC 20546-0001	Technical Paper
	14. Sponsoring Agency Code

15. Supplementary Notes

Mordechay Karpel: NRC-NASA Resident Research Associate, now at Technion-Israel Institute of Technology.

Sherwood Tiffany Hoadley: Langley Research Center, Hampton, Virginia.

16. Abstract

The minimum-state method for rational approximation of unsteady aerodynamic force coefficient matrices, modified to allow physical weighting of the tabulated aerodynamic data, is presented. The approximation formula and the associated time-domain, state-space open-loop equations of motion are given, and the numerical procedures for calculating the approximation matrices, with weighted data and with various equality constraints, are described. Two data weighting options are presented. The first weighting is for normalizing the aerodynamic data to the maximum unit value of each aerodynamic coefficient. The second weighting is one in which each tabulated coefficient, at each reduced frequency value, is weighted according to the effect of an incremental error of this coefficient on aeroelastic characteristics of the system. This weighting yields a better fit of the more important terms at the expense of less important ones. The resulting approximation yields a relatively low number of aerodynamic lag states in the subsequent state-space model. The formulation of this work forms the basis of the Minimum-State (MIST) computer program that is written in FORTRAN-77 for use on the VAX microcomputer and interfaces with NASA's Interaction of Structures, Aerodynamics, and Controls (ISAC) computer program. The program structure, capabilities, and interfaces are outlined in the appendixes, and a numerical example that utilizes Rockwell's Active Flexible Wing (AFW) model is given and discussed.

17. Key Words (Suggested by Authors(s))

s-plane approximation
Rational approximation of unsteady aerodynamics
Minimum-state method
Least-squares method
Physical weighting
Data weighting

18. Distribution Statement

Unclassified—Unlimited

Subject Category 02

19. Security Classif. (of this report)	20. Security Classif. (of this page)	21. No. of Pages	22. Price
Unclassified	Unclassified	45	A03

For sale by the National Technical Information Service, Springfield, Virginia 22161-2171